

1 **Analysis of genomic DNA from medieval plague victims suggests long-term effect of**  
2 ***Yersinia pestis* on human immunity genes**  
3  
4

5 Alexander Immel<sup>1,2,3</sup>, Felix M. Key<sup>1,4\*</sup>, András Szolek<sup>5\*</sup>, Rodrigo Barquera<sup>1\*</sup>, Madeline K.  
6 Robinson<sup>6</sup>, Genelle F. Harrison<sup>6</sup>, William H. Palmer<sup>6</sup>, Maria A. Spyrou<sup>1,3</sup>, Julian Susat<sup>2</sup>, Ben  
7 Krause-Kyora<sup>2</sup>, Kirsten I. Bos<sup>1,3</sup>, Stephen Forrest<sup>3</sup>, Diana I. Hernández-Zaragoza<sup>1,7</sup>, Jürgen  
8 Sauter<sup>8</sup>, Ute Solloch<sup>8</sup>, Alexander H. Schmidt<sup>8</sup>, Verena J. Schuenemann<sup>3,9</sup>, Ella Reiter<sup>3,9</sup>, Madita  
9 S. Kairies<sup>10</sup>, Rainer Weiß<sup>11</sup>, Susanne Arnold<sup>11</sup>, Joachim Wahl<sup>10,11</sup>, Jill A. Hollenbach<sup>12</sup>, Oliver  
10 Kohlbacher<sup>5,13,14,15,16</sup>, Alexander Herbig<sup>1,3</sup>, Paul J. Norman<sup>6#</sup>, and Johannes Krause<sup>1,17,3#</sup>

11  
12 <sup>1</sup> Max Planck Institute for the Science of Human History, Kahlaische Strasse 10, 07745 Jena, Germany

13 <sup>2</sup> Institute of Clinical Molecular Biology, Kiel University, Rosalind-Franklin-Strasse 12, 24105 Kiel, Germany

14 <sup>3</sup> Institute of Archaeological Sciences, University of Tübingen, Rümelinstrasse 23, 72070 Tübingen, Germany

15 <sup>4</sup> Max Planck Institute for Infection Biology, Charitéplatz 1, 10117 Berlin, Germany

16 <sup>5</sup> Applied Bioinformatics, Dept. for Computer Science, University of Tübingen, Sand 14, 72076 Tübingen, Germany

17 <sup>6</sup> Division of Biomedical Informatics and Personalized Medicine, and Department of Immunology & Microbiology,  
18 University of Colorado, CO 80045, USA

19 <sup>7</sup> Immunogenetics Unit, Técnicas Genéticas Aplicadas a la Clínica (TGAC), Mexico City, Mexico

20 <sup>8</sup> DKMS, Kressbach 1, 72072 Tübingen, Germany

21 <sup>9</sup> Institute of Evolutionary Medicine, University of Zurich, Winterthurerstrasse 190, 8057 Zurich, Switzerland

22 <sup>10</sup> Institute for Archaeological Sciences, WG Palaeoanthropology, University of Tübingen, Rümelinstrasse 23,  
23 72070 Tübingen, Germany

24 <sup>11</sup> State Office for Cultural Heritage Management, Stuttgart Regional Council, Berliner Strasse 12, 73728 Esslingen,  
25 Germany

26 <sup>12</sup> UCSF Weill Institute for Neurosciences, Department of Neurology, University of California, San Francisco, USA

27 <sup>13</sup> Institute for Bioinformatics and Medical Informatics, University of Tübingen, Sand 14, 72076 Tübingen,  
28 Germany

29 <sup>14</sup> Quantitative Biology Center, University of Tübingen, Auf der Morgenstelle 10, 72076 Tübingen,  
30 Germany

31 <sup>15</sup> Translational Bioinformatics, University Hospital Tübingen, Sand 14, 72076 Tübingen, Germany

32 <sup>16</sup> Biomolecular Interactions, Max Planck Institute for Developmental Biology, Max-Planck-Ring 5,  
33 72076 Tübingen, Germany

34 <sup>17</sup> Max Planck Institute for Evolutionary Anthropology, Deutscher Platz 6, 04103 Leipzig, Germany

35  
36 \*equal contribution

37 #corresponding authors  
38  
39

40 **Abstract**

41 **Pathogens and associated outbreaks of infectious disease exert selective pressure on human**  
42 **populations, and any changes in allele frequencies that result may be especially evident for**  
43 **genes involved in immunity. In this regard, the 1346-1353 *Yersinia pestis*-caused Black**  
44 **Death pandemic, with continued plague outbreaks spanning several hundred years, is one**  
45 **of the most devastating recorded in human history. To investigate the potential impact of *Y.***  
46 ***pestis* on human immunity genes we extracted DNA from 36 plague victims buried in a**  
47 **mass grave in Ellwangen, Germany in the 16<sup>th</sup> century. We targeted 488 immune-related**  
48 **genes, including *HLA*, using a novel in-solution hybridization capture approach. In**  
49 **comparison with 50 modern native inhabitants of Ellwangen, we find differences in allele**  
50 **frequencies for variants of the innate immunity proteins Ficolin-2 and NLRP14 at sites**  
51 **involved in determining specificity. We also observed that *HLA-DRB1\*13* is more than**  
52 **twice as frequent in the modern population, whereas *HLA-B* alleles encoding an isoleucine**  
53 **at position 80 (I-80+), *HLA C\*06:02* and *HLA-DPB1* alleles encoding histidine at position 9**  
54 **are half as frequent in the modern population. Simulations show that natural selection has**  
55 **likely driven these allele frequency changes. Thus, our data suggests that allele frequencies**  
56 **of *HLA* genes involved in innate and adaptive immunity responsible for extracellular and**  
57 **intracellular responses to pathogenic bacteria, such as *Y. pestis*, could have been affected by**  
58 **the historical epidemics that occurred in Europe.**

## 59 **Introduction**

60 Throughout evolution, humans have likely experienced multiple major episodes of infectious  
61 disease. Of exceptional virulence and lethality, *Yersinia pestis* has been responsible for at least  
62 three major plague pandemics during the last few millennia. Studies of ancient DNA have  
63 confirmed *Yersinia pestis* caused widespread infections in Europe from the Late Neolithic  
64 period, nearly 5,000 years ago, until the 18<sup>th</sup> century AD (Andrades Valtuena et al., 2016; Bos et  
65 al., 2016; Bos et al., 2011; Feldman et al., 2016; Keller et al., 2019; Namouchi et al., 2018;  
66 Rascovan et al., 2019; Rasmussen et al., 2015; Spyrou et al., 2018; Wagner et al., 2014).  
67 Historical records show the first pandemic began with the Justinianic Plague in the 6<sup>th</sup> century  
68 AD and lasted until the 8<sup>th</sup> century, the second began with the 1346-1353 Black Death and  
69 continued with thousands of local plague outbreaks until the 18<sup>th</sup> century (Biraben, 1976;  
70 Büntgen, Ginzler, Esper, Tegel, & McMichael, 2012) and the third pandemic started in China in  
71 the 19<sup>th</sup> century AD and spread the pathogen worldwide lasting up until the mid-20<sup>th</sup> century  
72 (Morelli et al., 2010; Politzer & WHO, 1954). Of the three recorded pandemics, the Black Death  
73 claimed up to half of the European population during its five-year period (Benedictow, 2004).  
74 Although *Y. pestis* is now absent from most of Europe, it still causes sporadic infections among  
75 humans in the Americas, Africa and Asia, usually transmitted by fleas from rodent populations  
76 that serve as plague reservoirs (Drummond et al., 2014; WHO, 2017). Although the lethality of  
77 plague is very high without treatment (WHO, 2017), it remains likely that specific individuals  
78 are protected from, or more susceptible to, severe disease through polymorphism in the  
79 determinants of natural immunity. In this case, any changes in allele frequencies that occurred  
80 during a given epidemic crisis could be evident as genetic adaptation and detectable in modern  
81 day individuals.

82  
83 There are multiple examples of natural selection affecting human immunity-related genes that  
84 can be attributed to challenge by pathogens. These examples include specific pathogens causing  
85 malaria, cholera or Lassa fever, or to wider differences in pathogen exposure between  
86 geographically discrete populations (Harrison et al., 2019; Karlsson et al., 2013; F. M. Key et al.,  
87 2014; Kwiatkowski, 2005; McManus et al., 2017; Sabeti et al., 2007; Voight, Kudravalli, Wen,  
88 & Pritchard, 2006; Wang, Kodama, Baldi, & Moyzis, 2006). The toll like receptors (TLRs) are  
89 innate immune proteins that detect the presence of specific pathogens to initiate an immune

90 response. Signatures of purifying selection have been identified within specific *TLR* genes that  
91 correlate with distinct pattern specificities of the encoded allotypes (Barreiro et al., 2009). In  
92 another example, recent signatures of positive selection in the *IFITM3* gene accompany  
93 differential abilities of the alternative variants to control pandemic H1N1 influenza A virus  
94 infection (Albright, Orlando, Pavia, Jackson, & Cannon Albright, 2008; Everitt et al., 2012). A  
95 final example of human genetic adaptation to pathogens is the 32 base pair deletion in the  
96 chemokine receptor *CCR5* (*CCR5-Δ32*), which prevents HIV from entering and infecting human  
97 T-cells (Dean et al., 1996). Although once postulated as a plague resistance allele (Stephens et  
98 al., 1998), there is little evidence for positive selection acting on *CCR5-Δ32* (Sabeti et al., 2006).  
99 By contrast, the Major Histocompatibility Complex (*MHC*), which encodes multiple immunity-  
100 related genes including the Human Leukocyte Antigen (*HLA*) molecules, does show evidence for  
101 recent positive and balancing selection and has established roles initiating and directing the  
102 immune response to infection (Klebanov, 2018; Parham & Moffett, 2013; Prugnolle et al., 2005;  
103 Trowsdale & Knight, 2013).

104  
105 Here, we extracted genomic DNA from 36 individuals who apparently died from plague (*Y.*  
106 *pestis*) in Ellwangen in Southern Germany during the 16<sup>th</sup> century. We also extracted DNA from  
107 50 modern day Ellwangen inhabitants. We then compared their frequency spectra for a large  
108 panel of immunity-related genes. We observed evidence for pathogen-induced changes in allele  
109 distributions for two innate pattern-recognition receptors and four *HLA* molecules. We propose  
110 that these frequency changes could have resulted from *Y. pestis* plague exposure during the 16<sup>th</sup>  
111 century.

112

## 113 **Results**

### 114 Archaeological and Anthropological Findings

115 Ellwangen is a small town of 27,000 inhabitants situated in South Germany near the border of  
116 Baden-Wuerttemberg and Bavaria. Ellwangen was founded in the 7<sup>th</sup> century AD, with only a  
117 few hundred inhabitants until modern times. The town was affected by multiple plague outbreaks  
118 during the 16th and 17th centuries (Ellwangen, 2007). From 2013 to 2015 an excavation took  
119 place in Ellwangen during the restoration of the town's market square (Figure 1). Three mass  
120 graves were discovered with a total of 101 inhumated remains (Supplementary Figure 1A).

121 Consistent with 16<sup>th</sup> century bubonic plague predominantly affecting children (Bowsky, 1971;  
122 Clouse, 2002; Cohn, 2003) only 23 of the individuals had reached adult age (Supplementary  
123 Note 1). The individuals were buried close to each other and there was little sediment between  
124 the distinct layers. The proximity, as well as radiocarbon dating, suggests that all three mass  
125 burials were created during the same epidemic crisis event during the 16<sup>th</sup> century  
126 (Supplementary Figure 1B). Genomic DNA from *Y. pestis* was identified previously from 13 of  
127 the individuals, and the complete genome of a strain consistent with the era was reconstructed  
128 from one of them (Spyrou et al., 2019; Spyrou et al., 2016). We also performed shotgun  
129 sequencing directly on DNA libraries prepared from tooth samples of 30 distinct individuals, and  
130 pathogen screening using the metagenomic alignment tool MALT (Vågane et al., 2018)  
131 identified reads matching to *Y. pestis* in 25 of them, with aDNA characteristic terminal  
132 substitutions in samples with sufficient coverage (Supplementary Table 1), confirming that the  
133 reads are of ancient DNA origin. With exception of one sequence read of Hepatitis B Virus in  
134 one of the petrous bone samples (ELW012), no evidence of other pathogens was detected.  
135 Additional archaeological and anthropological findings suggest little physical trauma, albeit poor  
136 health condition prior to death, which can likely be considered as normal health and nutrition  
137 status for people living in that time period (Supplementary Note 1). Taken together, these  
138 findings strongly suggest that these individuals were victims of a single *Y. pestis* plague outbreak  
139 that occurred during the 16<sup>th</sup> century.

140

#### 141 *The 16<sup>th</sup> century Ellwangen plague victims display genetic similarity with modern inhabitants*

142 From the 16<sup>th</sup> century mass grave site in Ellwangen, we successfully extracted DNA from 40  
143 petrous bones (Supplementary Figure 1C) and four teeth. DNA of sufficient quality and quantity  
144 for genome wide sequence analysis was obtained from all samples. An average of 1.76 million  
145 unique, human genome reads per individual was generated by shotgun sequencing  
146 (Supplementary Data 1A). Kinship analysis revealed three pairs of individuals to be first-degree  
147 relatives (Supplementary Data 1B, Supplementary Figure 2). In order to obtain the most accurate  
148 frequency distributions, one in each pair of the directly related individuals was removed from the  
149 allele frequency calculations. In these cases, the individual having the lowest yield of sequence  
150 reads was excluded (Material and Methods). In addition, one individual who was second-degree  
151 related to two of the other individuals was also excluded (ELW030). We also obtained genomic

152 DNA samples from 51 contemporary inhabitants of Ellwangen and shotgun-sequenced them  
153 with an average of 2.74 million unique human genome reads per individual (Supplementary Data  
154 1A). Here, we identified a single pair of first-degree relatives and removed one individual. In  
155 order to test whether the two cohorts derive from a single continuous population, we tested for  
156 population genetic similarity using Principle Component Analysis (PCA) (Patterson, Price, &  
157 Reich, 2006) and ADMIXTURE analysis (Alexander, Novembre, & Lange, 2009). Showing that  
158 the 16<sup>th</sup> century and modern groups indeed are genetically very similar, we found that the 16<sup>th</sup>  
159 century Ellwangen plague victims form a tight cluster in PCA space, which overlaps with the  
160 modern inhabitants (Figure 2A). This finding is bolstered by the highly similar genetic ancestry  
161 composition of the two groups as illustrated by their population admixture proportions (Figure  
162 2B). This latter finding is important because recent demographic changes could alter allele  
163 frequencies of the modern compared with the 16<sup>th</sup> century group (Hellenthal et al., 2014).

164

#### 165 Two immunity-related genes harbor strongly differentiated SNPs

166 In order to compare the allele spectra of immunity-related genes in the 16<sup>th</sup> century *Y. pestis*  
167 plague victims with modern-day inhabitants of Ellwangen, we developed an in-solution  
168 hybridization capture approach to enrich for 488 human genes implicated in immunity  
169 (Supplementary Table 2). This approach allowed us to specifically target the genes of interest  
170 while reducing the amount of sequencing required, leading to an average of 308 times more  
171 reads on target compared to undirected genome wide sequencing (Supplementary Figure 3). We  
172 applied this ‘immunity capture’ method to all 16<sup>th</sup> century and modern DNA samples. The  
173 targeted genes were covered with a mean read depth of 55.8 (Supplementary Data 2). We  
174 investigated the allele spectra of the 488 immunity-related genes by leveraging a branching  
175 statistic, *Differentiation with Ancestral (DAnC)* (F.M. Key, Fu, Romagné, Lachmann, & Andrés,  
176 2016). *DAnC* is calculated per site and uses derived allele frequency estimates across three  
177 populations; 16<sup>th</sup> century and modern Ellwangen, and a non-European outgroup (we used Han  
178 Chinese from Beijing (Abecasis et al., 2012)). *DAnC* scores can range from -1 to +1, and those in  
179 the respective far tails of the distribution identify candidates for simulation studies that could  
180 indicate positive selection has occurred. We established the expected distribution of *DAnC* scores  
181 (Supplementary Data 3) under neutrality through simulations using a human demographic model  
182 (Gravel et al., 2011).



183

184 In our analysis, the distribution of *DAnc* scores closely matches between the simulated and test  
185 data (Supplementary Figure 4, Supplementary Table 3). In the far tail of the distribution  
186 (>99.9%) we observed three SNPs, two in the Ficolin-2 (FCN2) gene and one in the NOD-like  
187 receptor purine domain containing 14 (NLRP14) gene (Table 1) also corresponding to the  
188 greatest  $F_{ST}$  values among the 488 genes for the same three SNPs (Supplementary Data 4).  $F_{ST}$  is  
189 an established measure for population differentiation and corrects for expected heterozygosity  
190 and sampling error (Weir & Cockerham, 1984). However, due to the ascertainment of SNPs,  
191 which are not representative of the whole genome, the far tail of the observed *DAnc* or  $F_{ST}$   
192 distribution is no evidence alone for positive selection. Alternatively, we compared the fraction  
193 of SNPs observed in the far tail of the simulated and test distribution, which suggest no  
194 enrichment of SNPs in our test data and thus no evidence for positive selection using the data at  
195 hand (Supplementary Table 3). Further analyses using a larger sample size and whole genome  
196 data is necessary in order to understand the role of positive selection due to historic epidemics.

197

198 The identified SNPs of FCN2 are a 5' UTR promoter variant [rs17514136 (-4 A to G)] and one  
199 coding change variant [rs17549193 (717 C to T; 236 Thr to Met)]. The UTR and coding change  
200 variants occur in complete linkage disequilibrium ( $\Delta' = 1.0$ ,  $R^2 = 0.9$ ), and appear to represent a  
201 single haplotype that has risen in frequency in the modern population. Interestingly, FCN2 binds  
202 to specific molecules on the surface of bacteria, triggering the complement pathway to neutralize  
203 the pathogen (Hoang et al., 2011; Luo et al., 2013). The promoter variant is associated with  
204 increased serum concentration of FCN2 (Cedzynski et al., 2007), whereas polymorphism at  
205 residue 236 (rs17549193) affects binding to the target bacteria (Hummelshoj et al., 2005).  
206 Similarly, NLRP14 belongs to inflammasome complex proteins, which are intracellular pattern  
207 recognition receptors that trigger local and systemic responses to microbial invasion (Martinon,  
208 Burns, & Tschopp, 2002). Inflammasomes are implicated in the immune response to *Yersinia*  
209 infection, amongst other pathogens (Philip, Zwack, & Brodsky, 2016; Vladimer, Marty-Roix,  
210 Ghosh, Weng, & Lien, 2013). The NLRP14 SNP is a coding change variant (rs10839708 [2745  
211 G to A: 808 Glu-Lys]) that occurs in the leucine-rich repeat (LRR) domain, which in related  
212 molecules controls the ligand specificity (Inohara, Chamailard, McDonald, & Nunez, 2005).  
213 Thus, in summary we show immune-related genes have no significant frequency changes

214 between 16<sup>th</sup> century *Y. pestis* victims and modern Ellwangen inhabitants.

215

### 216 No evidence for role of CCR5-Δ32 in protection from *Y. pestis* infection

217 We investigated the Δ32 deletion in the CCR5 locus (chr3:46414947-46414978), which was  
218 included in our target regions because this mutation has previously been suggested as protective  
219 from the plague. We found that CCR5-Δ32 has a frequency of 16.6% in the 16<sup>th</sup> century  
220 compared to 10.8% in the modern individuals (p=0.27) and 11.2% in Germany (Supplementary  
221 Data 5A and 5B, Supplementary Data 6A, Table 2). Consistent with epidemiological modeling  
222 and lack of evidence that CCR5 can serve as a *Y. pestis* receptor (Galvani & Slatkin, 2003) this  
223 finding suggests that the CCR5-Δ32 mutation provided no protection from *Y. pestis*. Similarly  
224 we also investigated SNPs *rs4986790*, *rs4986791* within the gene *TLR4* previously suggested to  
225 be associated with resistance to *Y. pestis* (Al Nabhani, Dietrich, Hugot, & Barreau; Laayouni et  
226 al., 2014). However, we did not find any significant differences in their respective frequencies  
227 (Supplementary Table 4).

228

### 229 Natural selection has increased HLA-DRB\*13 and reduced HLA-B\*51 and -C\*06 frequencies in 230 modern individuals

231 With more than 28,000 distinct alleles described (Robinson et al., 2015), HLA molecules are  
232 encoded by the most polymorphic gene complex in humans. When human populations are  
233 exposed to novel diseases through contact with populations or environments they had not  
234 encountered previously, changes in *HLA* allele frequencies can occur rapidly (Lindo et al., 2016;  
235 Patin et al., 2017). Consequently, the signatures of balancing selection in the genomic region that  
236 contains *HLA* are consistently the strongest in the genome (Quintana-Murci, 2019; Sabeti et al.,  
237 2006), and specifically correspond to amino acid residues that bind peptide fragments derived  
238 from pathogens (Bjorkman & Parham, 1990). Significant shifts in *HLA* allele frequencies can  
239 thus reveal evidence of natural selection for specific pathogen resistance. We were able to  
240 identify *HLA class I* (-A, -B, -C) and *HLA class II* (-DPA1, -DPB1, -DQA1, -DQB1 and -DRB1)  
241 genotypes from all of the 16<sup>th</sup> century and modern inhabitants of Ellwangen. We observed a total  
242 of 86 distinct *HLA class I* alleles, 66 distinct *HLA class II* alleles and 168 distinct *HLA*  
243 haplotypes (Supplementary Data 6B). The most frequent haplotype (*HLA-*  
244 *A\*01:01~B\*08:01~C\*07:01~DRB1\*03:01*) is the same in both groups and is also the most



245 common and widespread across Europe today (Darke et al., 1998; Dunne, Crowley, Hagan,  
246 Rooney, & Lawlor, 2008; Johansson, Ingman, Mack, Ehrlich, & Gyllensten, 2008; Nowak et al.,  
247 2008; Pingel et al., 2013). Thus the diversity and composition of *HLA* haplotypes appears as  
248 expected for Northern European populations (Alfirevic et al., 2012), and we did not observe any  
249 significant differences in their frequencies between the 16<sup>th</sup> century and modern individuals.

250  
251 By contrast to the haplotype distributions, on examining the individual *HLA class I* genes, we  
252 observed that the *B\*51:01* allele of *HLA-B* decreased from 15.3% in the 16<sup>th</sup> century Ellwangen  
253 plague victims to only 6.0% ( $p=0.04$  ( $p$ -corrected = NS);  $DANc= -0.093$ ) in the modern  
254 Ellwangen population (Table 3, Supplementary Data 4, Supplementary Data 5A). Similarly, the  
255 *C\*06:02* allele of *HLA-C* decreased from 13.9% to 5% ( $p=0.04$  ( $p$ -corrected = NS);  $DANc=$   
256  $0.053$ ). *HLA-B\*51:01* and *-C\*06:02* are not in linkage disequilibrium in either population  
257 (Supplementary Data 6B), and so these two observations are independent. In addition, although  
258 there were no significant frequency differences observed for any *HLA class II* alleles as  
259 determined at two-field resolution, we observed that all allotypes present representing the DR13  
260 serological group (Holdsworth et al., 2009) were at substantially lower frequency in the 16<sup>th</sup>  
261 century than modern Ellwangen population. Accordingly, by considering them together, there  
262 was an increase in *DR13* frequency from 5.6% in the 16<sup>th</sup> century to 17.0% in the modern  
263 individuals ( $p=0.026$ , Table 3, Supplementary Data 5A). Repeating this analysis for all the major  
264 *DRB1* lineages present (Holdsworth et al., 2009), showed *DRB1\*13* as the only allotype  
265 differing in frequency between the two groups (Table 3). We used Wilson Score Interval  
266 estimation of the 95% binomial confidence interval. The 95% CI of *HLA-B\*51:01* was 0.09 –  
267 0.25 (observed = 0.06), the 95% CI of *HLA-C\*06:02* was 0.08 – 0.24 (observed = 0.05), and  
268 *DRB1\*13* was 0.02 – 0.13 (observed = 0.16). Thus, for each of the three *HLA* allotypes showing  
269 distinctions between modern and 16<sup>th</sup> century inhabitants of Ellwangen, the observed modern  
270 allele frequencies are outside the 95% binomial confidence intervals surrounding sampling of the  
271 16<sup>th</sup> century allele frequencies. We further validated these findings by comparing the *HLA* allele  
272 frequencies observed in the Ellwangen individuals with a large panel ( $N=8,862$ ) of unrelated  
273 bone marrow donor registry volunteers gathered from all of Germany (Supplementary Data 5B).  
274 Whereas there were no significant allele frequency differences when comparing modern  
275 inhabitants of Ellwangen with modern Germany as a whole, we observed significantly lower

276 frequencies of *B\*51:01* in modern Germany (5.5%) than the Ellwangen plague victims (15.3%),  
277 when applying a pairwise proportion test ( $p=0.005$ ;  $DANc=-0.098$ ). We also observed  
278 differences in *HLA-C\*06* and *DRB1\*13* between the plague victims and modern Germany, but  
279 these were not statistically significant (Supplementary Data 5B).

280  
281 To distinguish if the changes in frequencies of *B\*51:01*, *C\*06:02* and *DRB1\*13:01* were more  
282 likely to be due either to natural selection or genetic drift we performed forward time simulations  
283 by starting from the observed polymorphisms in the 16<sup>th</sup> century Ellwangen and modelling  
284 neutrality for the last 500 years. This way it was possible to start from reasonable levels of  
285 genetic variation without the necessity to determine the impact of ancient selection on HLA and  
286 episodic turnover of HLA alleles. Moreover, this way each allotype could be tested individually.  
287 Again, we observed an overall concordance between median frequencies of the simulated neutral  
288 alleles and the modern Ellwangen allele frequencies, as is expected under genetic drift. By  
289 contrast, the allele frequencies of *B\*51:01*, *C\*06:02* and *DRB1\*13:01* observed for modern  
290 inhabitants of Ellwangen were in the extreme tails of their respective distributions ( $p^{sim}=0.006$ ,  
291  $0.004$ ,  $<0.001$ , respectively, Figure 3), suggesting natural selection likely drove the change in  
292 these allele frequencies. A similar significant shift was observed when we considered DR13  
293 broadly ( $p^{sim}<0.001$ ). To quantify the selection coefficient ( $s$ ) responsible for these changes, we  
294 performed the simulations incorporating selection, mirroring the timeline of the plague, across a  
295 range of  $s$  values. We identified an  $s$  equal to  $-0.25$  was most likely to produce the observed  
296 decrease in *B\*51:01* alleles as well as an  $s$  equal to  $-0.27$  in case of *C\*06:02*. An  $s$  of  $0.37$  was  
297 most likely to cause the increase in *DRB1\*13:01* (Supplementary Figure 5). Notably, these  
298 values are within the range of previously reported values of  $s$  acting on MHC (Radwan, Babik,  
299 Kaufman, Lenz, & Winternitz, 2020).

300  
301 *Higher incidence of KIR3DL1 interaction with HLA-B in plague victims than modern inhabitants*  
302 *of Ellwangen*

303 The binding specificity of HLA allotypes, and thus their function and distinctiveness, is  
304 determined by specific amino acid residues in the alpha-helix of the molecule. Polymorphism of  
305 these amino acid residues is associated with autoimmune diseases and response to pathogens  
306 (Achkar et al., 2012; Hammer et al., 2015; Hollenbach et al., 2019; Sun et al., 2018). We

307 identified three of these residues having significant ( $p < 0.05$ ) differences in frequency between  
308 the 16<sup>th</sup> century victims and modern individuals (Supplementary Data 7A). We observed  
309 histidine (H) at position 9 of HLA-DPB1 to be approximately three times more frequent in the  
310 16<sup>th</sup> century (13%) than the modern (4%) individuals ( $p = 0.03$  ( $p$ -corrected = NS); DANc = 0.13 );  
311 Supplementary Data 7A). We also observed isoleucine (I) at position 80 (I-80) in HLA-B twice  
312 as frequently in the 16<sup>th</sup> century (28%) than in the modern individuals (15%) ( $p = 0.04$  ( $p$ -  
313 corrected = NS); DANc = 0.28), and aspartic acid (D) at position 114 in HLA-C more frequently  
314 in the 16<sup>th</sup> century (85%) than the modern (70%) individuals ( $p = 0.02$  ( $p$ -corrected = NS);  
315 DANc = -0.062); Supplementary Data 7A). Residue D-114 is located in the outward-facing  
316 groove of HLA-C and its variation can directly affect the sequence of endogenous peptides able  
317 to bind (Di Marco et al., 2017). Since *HLA-B* alleles encoding I-80 are most commonly observed  
318 on haplotypes that also have *HLA-C* alleles that encode D-114 (Cao et al., 2001), it is likely that  
319 the observed frequency difference at this position is driven by linkage disequilibrium with *HLA-*  
320 *B*. *HLA-B*\*27:02, -B\*38:01, -B\*49:01, -B\*51:01, -B\*52:01, -B\*57:01 and -B\*58:01 are all I-  
321 80<sup>+</sup> allotypes that are more frequent in the 16<sup>th</sup> century than the modern inhabitants of Ellwangen  
322 (Supplementary Data 7B and 7C), together accounting for the observed difference in I-80  
323 frequency (Table 3). Thus, it is likely that the significant difference in frequencies we observed  
324 for *HLA-B*\*51:01 can be attributed to the fact that it possesses an isoleucine at position 80. We  
325 next tested whether the observed frequency changes in *HLA-DPB1* H-9 and *HLA-B* I-80 were  
326 more likely due to genetic drift or natural selection, using neutral forward genetic simulations as  
327 above. In both cases, we found these allele frequency shifts were unlikely to be observed unless  
328 natural selection was included in the model (*HLA-DPB1* H-9  $p^{sim} = 0.014$ , *HLA-B* I-80  
329  $p^{sim} = 0.002$ ).

330  
331 *KIR* genes encode surface proteins on natural killer (NK) cells whose interaction with HLA class  
332 I molecules can determine the outcome of NK cell responses (Guethlein, Norman, Hilton, &  
333 Parham, 2015). For example, polymorphism of residue 80 in *HLA-B* controls its ability to bind  
334 to KIR3DL1, with I-80 defining ligand specificity and permitting the strongest interaction  
335 (Saunders et al., 2015). We therefore sought to determine whether the observed high frequency  
336 of *HLA-B* I-80<sup>+</sup> alleles in the 16<sup>th</sup> century samples affects the frequency of *HLA-B* interaction  
337 with KIR3DL1. The *KIR* region varies by gene content (Uhrberg et al., 1997), and we were able



369 observed allele frequency differentiation. Both of these molecules are pattern recognition  
370 receptors that bind specific pathogen-derived components to initiate the inflammation response;  
371 Ficolin-2 does this extracellularly, and NLRP14 intracellularly. Ficolin-2 promotes phagocytosis  
372 of pathogenic bacteria (Hoang et al., 2011; Luo et al., 2013). Interestingly, we observed two  
373 SNPs of known direct functional effect to be in strong LD, forming a single haplotype that is  
374 elevated in frequency in the modern compared to the 16<sup>th</sup> century individuals. This haplotype  
375 both increases serum concentration and alters the binding properties of Ficolin-2 (Cedzynski et  
376 al., 2007; Hummelshoj et al., 2005), which makes it a good candidate for providing improved  
377 resistance to *Y. pestis* infection. On the other hand, less is known about NLRP14, which has  
378 similar domain organization to other inflammasome proteins. Inflammasomes act to trigger  
379 inflammation as well as self-destruction of infected cells (Lamkanfi & Dixit, 2014) and have  
380 been identified recently as important mediators of the immune response to *Y. pestis* (Park et al.,  
381 2020). Interestingly, the same variant we observed at lower frequency in modern individuals than  
382 plague victims (K-808) was identified at high frequency due to positive selection in the Human  
383 Genome Diversity-Project populations from East-Asia (Vasseur et al., 2012). Similar  
384 inflammasome molecules, including NLRP3 and NLRP12, are known to respond to *Y. pestis*  
385 (Vladimer et al., 2013; Vladimer et al., 2012), but may also be exploited by bacteria to inhibit  
386 immunity (Anand et al., 2012; Philip et al., 2016; Zaki, Man, Vogel, Lamkanfi, & Kanneganti,  
387 2014). K-808 is located in the LRR domain of NLRP14 and influences ligand specificity.  
388 Therefore, the fluctuating frequencies of the variants at this position point to an evolutionary  
389 battle between host and pathogen (Abi-Rached, Dorigi, Norman, Yawata, & Parham, 2007).  
390 Functional tests are thus required to determine if mutation at residue 808 permits recognition of  
391 any components of *Y. pestis*.

392 On examination of *HLA* alleles we observed candidates for natural selection of human adaptive  
393 immune responses. HLA class I and II are cell surface molecules that bind to peptides derived  
394 from intracellular or extracellular proteins, respectively. To trigger and drive the adaptive  
395 immune response, these peptides are presented by the HLA molecules to T-cells. Antibody  
396 production is elicited through highly polymorphic HLA class II molecules, HLA-DP, -DQ, and -  
397 DR, presenting pathogen-derived peptides to CD4<sup>+</sup> T-cells (Neefjes, Jongma, Paul, & Bakke,  
398 2011). Direct killing of infected cells can occur when any of three highly polymorphic HLA  
399 class I molecules, HLA-A, -B or -C, presents pathogen-derived peptides to cytotoxic CD8<sup>+</sup> T-

400 cells (Doherty & Zinkernagel, 1975). The *HLA-DRB1\*13* allelic group increased in frequency  
401 from 5.6% in the plague victims to 17% in the modern Ellwangen individuals and 12% in the  
402 German bone marrow donors, potentially indicating antibody-driven protection from the plague  
403 for individuals having this allotype. *HLA-DRB1\*13* is associated with resistance to *M.*  
404 *tuberculosis* (Dubaniewicz, Lewko, Moszkowska, Zamorska, & Stepinski, 2000). Similar to *Y.*  
405 *pestis*, *M. tuberculosis* can invade and survive within macrophages (Pieters, 2008). Macrophages  
406 express high levels of HLA class II and are cells that are specialized for presenting peptides to  
407 CD4+ T cells to initiate antibody production. These HLA class II molecules can present antigens  
408 from intracellular pathogens, such as *M. tuberculosis* (Ankley, Thomas, & Olive, 2020). Thus,  
409 the same adaptive immune pathway triggered by *HLA-DRB1\*13* that provides resistance to *M.*  
410 *tuberculosis*, might also provide resistance to *Y. pestis*.

411  
412 Some HLA class I allotypes interact with killer-cell immunoglobulin-like receptors (KIRs) to  
413 modulate the function of Natural Killer (NK) cells, which are essential components of innate  
414 immunity, providing front-line defense against infection (Guethlein et al., 2015; Long, Kim, Liu,  
415 Peterson, & Rajagopalan, 2013). The *KIR* locus varies by gene content (Uhrberg et al., 1997;  
416 Wilson et al., 2000) and is located on a separate chromosome (chr19) to HLA (chr6).  
417 Combinatorial diversity of HLA class I and KIR allotypes directly impacts NK cell responses to  
418 infection (Bashirova, Martin, McVicar, & Carrington, 2006; Parham & Moffett, 2013). We  
419 observed a lower frequency of the HLA-B allotypes that can interact with KIR3DL1 in the  
420 modern individuals than we did in the plague victims, suggesting this combination could have  
421 been disadvantageous for individuals infected with *Y. pestis*. KIR3DL1 is an inhibitory receptor  
422 that enables NK cells to respond strongly to changes in HLA expression by infected cells  
423 (Boudreau & Hsu, 2018; Saunders et al., 2015) (Gumperz, Litwin, Phillips, Lanier, & Parham,  
424 1995). Finally, we observed a marked decrease in the frequency of *HLA-C\*06:02* when  
425 comparing the 16<sup>th</sup> century and modern Ellwangen populations. *HLA-C\*06:02*, which also  
426 interacts strongly with KIR (Hilton et al., 2015), is strongly associated with psoriasis (Ogawa &  
427 Okada, 2020), an immune-mediated disease. These observations implicate excess collateral  
428 damage caused by NK cells responding to infection (Guo, Patil, Luan, Bohannon, & Sherwood,  
429 2018; Kim et al., 2008), as a potential mechanism of pathology.

430



431 A limitation of this study is the relatively small sample size of 36 plague victims from the 16<sup>th</sup>  
432 century. As suggested by our effect size analyses (Supplementary Figure 7), with the given  
433 sample size only large effects ( $w = 0.40 - 0.45$ ) can be detected, and therefore, the observed  
434 frequency changes do not withstand multiple testing correction. Thus, it also remains possible  
435 that the signals of selection we detected for some variants are caused by drift and/or sampling  
436 biases, and, on the other hand, some other variants under selection were potentially not targeted  
437 through this approach. Increasing the sample size in future studies will allow addressing this  
438 caveat. Moreover, all tested individuals are 16<sup>th</sup> century late plague victims, and it remains  
439 possible that stronger selection signatures could be observed when analyzing individuals who  
440 died of plague in earlier pandemics. Importantly, further cohorts of *Y. pestis* victims are required  
441 to verify the observations in this study in different geographic contexts, and also whether the  
442 associations with the above-mentioned immunity genes are specific to the plague or might be  
443 caused by other pathogens (Galvani & Slatkin, 2003). Furthermore, the demographic model we  
444 used for simulation of natural selection is fitted to the CEU population (Central Europeans from  
445 Utah) (Gravel et al., 2011) and assumes an exponential population growth. However, the CEU  
446 population might have had a different demographic history than Ellwangen. It cannot, therefore,  
447 be ruled out that the results from our analysis of natural selection may be inaccurate, if  
448 Ellwangen has undergone stronger genetic drift than CEU. Nevertheless, our simulation results  
449 provide preliminary evidence for natural selection as the main driving agent for the decrease of  
450 frequencies in HLA-C\*06:02, HLA-B\*51:01 (and other HLA-B I-80<sup>+</sup> alleles), and HLA-DPB1-  
451 H9 on the one hand, and the frequency-increase in HLA-DRB1\*13 on the other hand. We note  
452 that the frequency changes we observed are based on simulations of episodic selection and could  
453 also be derived through alternative scenarios, including constant selection pressure (e.g.  $s$  of -  
454 0.012 B\*51, -0.014 C\*06, 0.06 DRB1\*13); (data not shown), or other epidemic challenges, such  
455 as smallpox or tuberculosis, occurring since the 16<sup>th</sup> century. However, we did not find evidence  
456 of smallpox or tuberculosis in the plague victims' DNA. Comparison with non-plague victims  
457 from the same time period will be necessary to definitively answer this question. Our results do  
458 not provide support for the proposition that evolution of human immunity drove reduction of *Y.*  
459 *pestis* virulence and its disappearance from Europe (Ell, 1984). Instead, we provide first evidence  
460 for evolutionary adaptive processes that might be driven by *Y. pestis* and may have been shaping  
461 certain human immunity-relevant genes in Ellwangen and possibly also in Europe. As the earliest

462 victims of *Y. pestis* in Europe were already present in the Late Neolithic (Andrades Valtuena et  
463 al., 2016; Rascovan et al., 2019; Rasmussen et al., 2015) and Europeans were intermittently  
464 exposed to plague for almost 5,000 years, it is possible that relevant immunity alleles had already  
465 been pre-selected in the European population long ago and maintained by standing variation  
466 (Ralph & Coop, 2015) but recently became selected through epidemic events. Whilst *Y. pestis*  
467 seems a likely culprit, this remains to be determined through replication cohorts and further  
468 functional analyses.

469  
470  
471  
472  
473  
474

## 475 **Material and Methods**

### 476 Anthropological analyses

477 Anthropological analyses on the skeletal remains were conducted in the Institute of  
478 Paleoanthropology, University of Tübingen. Diseases of the periodontium and the teeth,  
479 nonspecific stress markers and deficiencies, degenerative transformations, inflammatory bone  
480 changes, and trauma were recorded (Supplementary Note 1). The body height of the adult  
481 individuals was reconstructed and the growth course of the sub adult individuals was analyzed  
482 (Kairies, 2015).

483

### 484 C14-Dating of the archaeological remains from Ellwangen

485 Acceleration Mass Spectrometry Radiocarbon (AMS-C14) dating was conducted at the Curt-  
486 Engelhorn Center for Archaeometry in Mannheim. Calibration was performed based on the  
487 INTCAL13 and the SwissCal 1.0 calibration curves.

488

### 489 DNA extraction

490 Petrous pyramids were cut longitudinally in order to enable access to the bony labyrinth  
491 (Supplementary Figure 1C), which is the densest part of the mammalian body (Frisch, Sorensen,  
492 Overgaard, Lind, & Bretlau, 1998) and provides the highest endogenous DNA yields (Pinhasi et

493 al., 2015). After cleaning the surface on one side of the bony labyrinth with the drill bit,  
494 sampling was performed along the semicircular canal, which yielded 80-120 mg bone powder.  
495 DNA extraction was performed by guanidinium-silica based extraction (Rohland & Hofreiter,  
496 2007) using all the bone powder obtained. Tooth samples were cut in the middle, thus separating  
497 the crown from the root, followed by drilling into the dental pulp to produce bone powder (ca.  
498 100 mg). Saliva samples were obtained from 51 living Ellwangen citizens using *Whatman*  
499 *OmniSwab* cheek swabs. Samples were obtained only from individuals whose families have been  
500 resident in Ellwangen for at least four generations. Consent was given by the contributing  
501 persons and their samples were anonymized. Approval for the study was granted by the Ethics  
502 Committee of the Faculty of Medicine of the Eberhard Karls University and the University  
503 Hospital Tübingen. Isolation of genomic DNA was performed using the *QIAamp DNA Blood*  
504 *Mini Kit* following the *Qiagen* protocol.

505

#### 506 Preparation of libraries and sequencing

507 Overall strategy: Indexed libraries were generated from all samples and the sequencing was then  
508 performed in two stages. First, an aliquot of the full DNA library was subjected to whole genome  
509 sequencing. Then, a second aliquot was subjected to enrichment for selected immunity-related  
510 genes and subsequently sequenced.

511

512 Since our protocols for DNA extraction and library preparation are optimized for short-length  
513 ancient DNA, and in order to avoid potential bias through laboratory methods, we sheared the  
514 DNA extracted from modern individuals using ultrasonic DNA shearing to the same average  
515 length as the ancient DNA. Therefore, the modern DNA was sheared to an average fragment  
516 length of 75 bp using a *Covaris M220 Focused ultrasonicator*. DNA libraries, including sample-  
517 specific indices, were prepared using 20 µl of each extract following published protocols  
518 (Kircher, Sawyer, & Meyer, 2012; Meyer & Kircher, 2010). For the ancient samples, partial  
519 uracil-DNA-glycosylase treatment was first applied (Rohland, Harney, Mallick, Nordenfelt, &  
520 Reich, 2015). Sequencing was performed using an Illumina *Hiseq 4000* instrument with 75+8  
521 cycles in single-end mode.

522

523

524 Screening for pathogens

525 DNA samples were screened for their metagenome content using the alignment tool MALT  
526 version 0.3.8 (Vågene et al., 2018) and the metagenome analyzer MEGAN V6.11.4 (Huson,  
527 Auch, Qi, & Schuster, 2007) (Supplementary Table 1).

528  
529 Since petrous bone samples are not ideal for pathogen screening, we additionally accessed well-  
530 preserved tooth samples from 30 distinct 16th century plague victims. Teeth were not available  
531 from all individuals from whom we had obtained petrous bones, nor could they be  
532 unambiguously attributed to specific individuals. Sequencing libraries and shotgun sequencing  
533 were performed on the teeth following published protocols as described above.

534 MALT was used to align all pre-processed reads against a collection of all complete bacterial  
535 genomes obtained from NCBI (ftp.ncbi.nlm.nih.gov/genomes/refseq/bacteria, access  
536 12.03.2018). MALT was executed in BLASTN mode for bacteria using the following command:  
537 malt-run --mode BlastN --e 0.001 --id 95 --alignmentType SemiGlobal --index \$REF --inFile  
538 \$IN --output \$OUT (where \$REF is the MALT index). The e-value (--e) is a parameter that  
539 describes the number of hits that are expected to be found just by chance. The --id parameter  
540 describes the minimum percent identity that is needed for a hit to be reported. As the screening  
541 with MALT was performed on aDNA data the applied filters are not very stringent since we  
542 expect substitutions in organisms from ancient samples.

543 Reads assigned to the *Yersinia pestis* node and reads assigned to the nodes below, were extracted  
544 using the extract reads function in MEGAN. For subsequent verification blastn (version 2.7.1)  
545 was used to blast the extracted reads against *Yersinia pestis* (NC\_003143.1) and *Yersinia*  
546 *pseudotuberculosis* (NC\_010634.1). The following custom blast command was used:

547 blastn -db \$REF -query \$IN -outfmt "6 qseqid sseqid pident length mismatch gapopen qstart  
548 qend sstart send eval evalue bitscore gaps" (where \$REF is the reference genome and \$IN are the  
549 extracted reads from MEGAN).

550

551 Targeted sequencing of immunity-related genes

552 Indexed libraries containing 20 µl DNA each were amplified in 100 µl reactions in a variable  
553 number of one to seven cycles to reach the required concentration of 200 ng/µl for enrichment,  
554 followed by purification using *Qiagen MinElute* columns. Using an in-solution capture-by-

555 hybridization approach (Fu et al., 2013), DNA molecule fragments originating from immunity  
556 genes were enriched from the total DNA. The design and manufacture of the capture probes are  
557 described below. Sequencing was performed as above.

558

#### 559 DNA damage estimation

560 We performed an initial analysis of the merged data using the *EAGER* pipeline (Peltzer et al.,  
561 2016) as follows: reads were mapped to *hg19* (The Genome Sequencing Consortium, 2001)  
562 using the *aln* algorithm in *BWA 0.7.12* (H. Li & Durbin, 2010) with a seed length (k) of 32, the  
563 *samtools* mapping quality parameter “q” set to 30 and a reduced mapping stringency parameter  
564 “-n 0.01” to account for damage in ancient DNA. On average 2.2 million reads (51%) from the  
565 plague victims with an average length of 59 bp, and 4.2 million reads (91%) from the modern  
566 individuals with an average length of 68 bp, mapped uniquely to hg19 (Supplementary Data 1A).  
567 To assess the authenticity of the ancient DNA fragments, C to T misincorporation frequencies  
568 (Briggs et al., 2007) were obtained using *mapDamage 2.0* (Jonsson, Ginolhac, Schubert,  
569 Johnson, & Orlando, 2013). As expected from partial UDG-treatment (Rohland et al., 2015),  
570 ancient DNA sequences showed C to T substitutions at the first two positions of their 5’ ends and  
571 G to A substitutions at the 3’ ends (Supplementary Data 1A). The first two positions from the 5’  
572 end of the fastq-reads were trimmed off. The modern sample DNA sequence reads were not  
573 subjected to this trimming.

574

#### 575 Sex determination

576 Genetic sex was determined based on the ratio of sequences aligning to the X and Y  
577 chromosomes compared to the autosomes (Skoglund, Storå, Götherström, & Jakobsson, 2013).

578

#### 579 Final data collation

580 Contamination was estimated through examination of mitochondria sequences using the software  
581 *Schmutzi* (Renaud, Slon, Duggan, & Kelso, 2015), and in males additionally on the X-  
582 chromosomal level by applying *ANGSD* (Korneliussen, Albrechtsen, & Nielsen, 2014).  
583 Contamination estimates ranged between 1 and 3% on mitochondrial and between 0.2 and 2.9%  
584 on X-chromosomal level (Supplementary Data 1A). Datasets showing >8% contamination were  
585 excluded from further analyses.

586

587 Genotyping

588 SNPs were drawn at random at each position from a previously published dataset of 1,233,013  
589 SNPs (Haak et al., 2015; Lazaridis et al., 2014; Mathieson et al., 2015) in a pseudo-haploid  
590 manner using *pileupcaller* from the *sequenceTools* package (Lamnidis et al., 2018). Samples  
591 having fewer than 10,000 calls from a set of 1,233,013 SNPs were excluded. Forty-four datasets  
592 from ancient samples (40 from petrous bones and four from teeth) and 52 datasets from modern  
593 saliva samples remained.

594

595 Population genetic analyses

596 The genotype data from both Ellwangen populations were merged with a dataset of previously  
597 published West Eurasian populations genotyped on the aforementioned 1,233,013 SNPs  
598 (Mathieson et al., 2015) using the program *mergeit* from the *EIGENSOFT* package (Patterson et  
599 al., 2006). Principle Component Analysis (PCA) was performed using the software *smartpca*  
600 (Patterson et al., 2006). Admixture modelling was performed using the software ADMIXTURE  
601 (Alexander et al., 2009) with 65 West Eurasian populations from the *Affymetrix Human Origin*  
602 dataset, and the number of ancestral components ranging from K=3 to K=12. Cross-validation  
603 was performed for every admixture model and the model with the highest accuracy was  
604 determined by the lowest cross-validation error.

605

606 Kinship analysis

607 Kinship was assessed using three different software packages: *READ* (Monroy, Jose, Jakobsson,  
608 & Günther, 2017), *lcMLkin* (Lipatov, Sanjeev, Patro, & Veeramah, 2015) and *outgroup f3*  
609 statistics (Patterson et al., 2012). *READ* identifies relatives based on the proportion of non-  
610 matching alleles. *lcMLkin* infers individual kinship from calculated genotype likelihoods, and *f3*  
611 statistics can be used to identify relatives based on the amount of shared genetic drift. A pair of  
612 individuals was regarded related if evidence of relatedness was independently provided by at  
613 least two programs. For the modern population a first-degree relationship (parent-child or  
614 siblings) was detected by all three programs for EL1 and EL57. For the plague victims, evidence  
615 of a first-degree kinship was provided from all three programs for three pairs of individuals:  
616 ELW015 and ELW037, ELW016 and ELW017, and ELW036 and ELW039. Support from at



617 least two programs was given for second degree relatedness (grandparent-grandchild, uncle-  
618 nephew or first cousins) for two pairs: ELW021 and ELW030, and ELW007 and ELW039.  
619 Second- or higher-degree relatedness was suggested for the pair ELW030 and ELW034. Nine  
620 further observations of second-degree relationships were observed, but supported by only one  
621 program at a time and therefore not regarded as reliable kinship estimates (Supplementary Figure  
622 2). Individuals EL57, ELW017, ELW030, ELW037 and ELW039 were excluded from allele  
623 frequency calculations, since they constitute kinship “nodes” or “leaves” that would bias allele  
624 frequencies as they do not contribute to the total allele diversity.

625

### 626 Effect size analysis

627 Effect sizes were estimated and plotted in *G\*Power* 3.1.9.2 (Faul, Erdfelder, Lang, & Buchner,  
628 2007) based on the given sample size and a power of 0.8. Effect size analysis has shown that  
629 with the current sample size large to medium effects ( $w=0.45-0.4$ ) could be detected  
630 (Supplementary Figure 7).

631

### 632 Probe design for immune-capture

633 Enrichment of selected target genomic regions prior to sequencing can save sequencing costs and  
634 significantly reduce microbial DNA contaminants (Fu et al., 2016; Gnirke et al., 2009; Haak et  
635 al., 2015; Lazaridis et al., 2014; Mathieson et al., 2015). We therefore selected a set of 488  
636 different human genes representative of the innate and adaptive immune system (Supplementary  
637 Table 2). Exon sequences were extracted from the human genome build *hg19* (The Genome  
638 Sequencing Consortium, 2001) using the *RefSeqGene* records from the *NCBI/Nucleotide*  
639 database and then selecting “Highlight Sequence Features” and “Exon”. We added alternative  
640 alleles for *HLA*, *MIC*, *TAP* and *KIR*, which were obtained from the IMGT/HLA database  
641 (Robinson et al., 2015). For *HLA class I* and *KIR* genes the intronic regions were also included.  
642 For the *HLA* and *MIC* genes a set of 83 representative alleles with full-length gene sequences  
643 was chosen that encompasses the major serologically defined subclasses (Holdsworth et al.,  
644 2009) and covers 95% of the known polymorphism. To capture the remaining 5%, a set of 162 x  
645 160 bp consensus sequences was designed.

646 A 60 bp probe was designed at every 5 bp interval along the target sequence. The last (3') 8 bp  
647 of each generated sequence was replaced by a custom primer sequence, so that probes could be

648 amplified. The final 52 bp probe sequences were mapped to *hg19* using *RazerS3* (Weese,  
649 Holtgrewe, & Reinert, 2012) with minimum threshold of 95% identity. Duplicates and probe  
650 sequences that mapped more than 20 times were removed. This process resulted in a final set of  
651 322,667 unique probe sequences of 52 bp length. The probe set was tripled to complete capacity  
652 of the *Agilent* 1-million feature array. The probes were cleaved from the array and amplified  
653 using PCR (Fu et al., 2016). In summary, we generated 322,667 unique probes of 52 bp length  
654 using stepwise 5 bp tiling to cover a total of 3,355,736 bp. The final set of probe sequences is  
655 available in Supplementary Data 8. To validate the capture protocol, we used seven cell lines  
656 from the Immunogenetics and Histocompatibility Workshop (IHW) chosen to represent  
657 divergent HLA alleles that we had previously sequenced to full resolution (P. J. Norman et al.,  
658 2017). The results are shown in Supplementary Data 2.

659

#### 660 Analysis of the CCR5-Δ32 frequency

661 The CCR5 locus (chr3:46414947-46414978) was included in the target regions. To genotype  
662 CCR5 for wildtype (wt) and Δ32 alleles, the sequence data was remapped to *hg19* using *BWA-*  
663 *mem* with the mapping quality filter turned off. To generate genotypes, the CCR5 locus was  
664 visually inspected using the Integrative Genomics Viewer (Robinson et al., 2011).

665

#### 666 1000 Genome data for selection scan

667 We obtained the “low coverage” and “exome” aligned data for a set of 50 unrelated individuals  
668 for the East Asian population CHB (Han Chinese in Beijing, China) from the 1000 Genomes  
669 Phase 3 dataset (<ftp://ftp.1000genomes.ebi.ac.uk/vol1/ftp/phase3/data/>). The bam files were  
670 converted into *fastq* format using the *bamtobfastq* option from the software *bedtools* 2.28.0  
671 (Quinlan, 2014).

672

#### 673 Variant detection

674 We used *samtools mpileup* (Heng Li et al., 2009) for variant detection with a minimum mapping  
675 and base quality of 30 while ignoring indels (-q 30 -Q 30 -C 50 -t DP,SP -g --skip-indels), and  
676 used *bcftools* (Heng Li, 2011) for variant calling (-m -f GQ -O b). We considered only variants  
677 that were within the captured regions +/- 1,000 bp. Variants were kept when at least 10  
678 individuals had a genotype quality of 30 or higher as measured using *vcftools* (Danecek et al.,

2011). Resulting vcf-files were further annotated by adding the ancestral allele and dbSNP IDs  
 version 147. The ancestral allele was called as the most parsimonious based on 1000 Genomes  
 data (Abecasis et al., 2012) and a multiple species alignment (F.M. Key et al., 2016).

### *DAnc calculation*

For all variants shared across the Ellwangen data (modern and ancient) and 1000 Genomes CHB  
 population we calculated a *Differentiation with Ancestral (DAnc)* score (F.M. Key et al., 2016).  
*DAnc* is calculated per site, and uses derived allele frequency estimates to infer population-  
 specific allele frequency changes. Therefore, we inferred the derived allele frequency (DAF)  
 using the annotated ancestral allele for every site. Using the DAF we calculated *DAnc* scores per  
 site:

$$DAnc = |(ELW_{MOD} - CHB)| - |(ELW_{ANC} - CHB)|$$

For every site the resulting *DAnc* scores can range from -1 to +1. Invariable sites have a score of  
 0. A positive *DAnc* score indicates that the modern Ellwangen population has a different allele  
 frequency compared to the ancient Ellwangen population and the outgroup population, e.g. due  
 to recent positive selection. A negative *DAnc* score indicates that the ancient Ellwangen  
 population differentiates from both modern Ellwangen and the outgroup CHB.

### *Estimating F<sub>ST</sub> values*

We calculated F<sub>ST</sub> values for all variants using the (Weir & Cockerham, 1984) estimator  
 implemented in *vcf-tools* (Danecek et al., 2011). We report the empirical p-values, which were  
 obtained by comparing the F<sub>ST</sub> of all three candidate SNPs to the empirical distribution of F<sub>ST</sub>  
 scores from all other variants.

### *Simulation of neutral evolution*

In order to estimate the expected distribution of *DAnc* scores under neutral evolution, we  
 simulated the European demographic history, using a published model (Gravel et al., 2011) and  
 the simulation software *slim2* (Haller & Messer, 2017). The demographic model is based on  
 genome-wide data; we however had predominantly capture data from coding regions. To account

709 for increased drift in coding regions due to background selection, we reduced the effective  
710 population sizes using background selection coefficients (*B scores*) (F.M. Key et al., 2016). We  
711 estimated background selection for every genomic region captured using a published genome-  
712 wide map (McVicker, Gordon, Davis, & Green, 2009). The complete model including all  
713 parameters is available in Supplementary Data 9. We ran 100,000 simulations of genomic loci  
714 matched in length to the captured region and used the resulting variants to calculate the neutral  
715 expectation of the *D<sub>Anc</sub>* score distribution.

716

### 717 Simulation of natural selection

718

719 We performed 10,000 forward genetic simulations using *slim3* (Haller & Messer, 2019) to  
720 determine null distributions for neutral frequency changes over 500 years in Ellwangen for each  
721 HLA and KIR allotype. We used the sampled ancestral Ellwangen HLA and KIR allotype  
722 frequencies as input and simulated 20 generations, assuming a 25 year generation time (e.g.  
723 Gravel et al, 2011). We assumed a constant population growth rate of 1.085 per generation,  
724 resulting in growth from 5000 to approximately 25000 in Ellwangen. We explicitly modelled  
725 HLA and KIR allotypes, using linked binary identifiers to differentiate between alleles of a gene,  
726 and therefore assumed no new mutations or intragenic recombination. We calculated intergenic  
727 recombination rates per generation between *HLA* genes using a recent sex-averaged refined  
728 genetic map (Bhérier, Campbell, & Auton, 2017). We allowed free recombination between *HLA*  
729 and *KIR* regions (because they are on separate chromosomes). Specifically, we assumed the  
730 following number of crossovers per generation between each HLA gene. HLA-A/HLA-C:  $5.3e^{-3}$ ,  
731 HLA-C/HLA-B:  $1e^{-8}$ , HLA-B/HLA-DRB345:  $5.4e^{-3}$ , HLA-DRB345/HLA-DRB1:  $1e^{-8}$ , HLA-  
732 DRB1/HLA-DQA1:  $3.2e^{-5}$ , HLA-DQA1/HLA-DQB1:  $3.9e^{-7}$ , HLA-DQB1/HLA-DPA1:  $6.5e^{-3}$ ,  
733 and HLA-DPA1/HLA-DPB1:  $1e^{-8}$ . We calculated neutral frequency changes of each allotype.  
734 We conclude the frequency changes of an allotype is due to natural selection if the sampled  
735 modern day allotype frequency falls within the 0.5% extremes of the respective neutral  
736 distribution ( $p < 0.01$ ).

737 We re-implemented the neutral *slim3* models as described above, but included a non-zero *s*  
738 parameter for each HLA-allotype in question. For each selected allotype, we ran 100 simulations  
739 with a positive or negative *s* with an absolute value of 0.001, 0.01, 0.1, 0.2, 0.3, 0.4, 0.5, 0.6 or  
740 0.7. Mirroring the timeline of the European plague outbreak, allotypes were selected for 7

741 generations and then returned to neutrality. The reported  $s$  values were consistent with previous  
742 reported values of  $s$  acting on *MHC* genes (Radwan et al., 2020). We estimated the strength of  
743 natural selection by fitting a LOESS curve to the simulated relationship between  $s$  and allotype  
744 frequency and mapping the observed modern Ellwangen allotype frequency.

745

#### 746 *HLA typing of the Ellwangen individuals*

747 We applied the *OptiType* algorithm, which is a program that enables HLA genotyping from high-  
748 throughput sequence data. *OptiType* requires a minimum of a 12-fold coverage to reliably  
749 determine the HLA alleles present at two-field (distinct polypeptide sequences) resolution. We  
750 applied *OptiType* (Szolek et al., 2014) to identify HLA class I alleles, using a reference set of  
751 present-day HLA allele sequences and a required sequence identity of at least 97% for every  
752 alignment. We set no limit on the number of potential best matches during read mapping. We  
753 manually verified the results obtained by a development version of the upcoming *OptiType* 2.0  
754 package in order to determine HLA class II alleles. For every sample, the *OptiType* call having  
755 highest confidence was used.

756

#### 757 *Reconstruction of HLA haplotypes*

758 Haplotypes were assigned based on previously reported frequencies and linkage disequilibrium  
759 (LD) (Cao et al., 2001; González-Neira et al., 2004). Maximum-likelihood haplotype frequencies  
760 for alleles and two-point, three-point and four-point associations were estimated using an  
761 Expectation-Maximization (EM) algorithm provided by the computer program *Arlequin* ver. 3.5  
762 (Excoffier & Lischer, 2010).

763

#### 764 *Comparing allele and haplotype frequencies*

765 HLA allele frequencies were calculated from HLA-A, -B, -C, and -DRB1 sequence data of 8862  
766 potential stem cell donors registered with DKMS (German Bone Marrow Donor Registry) until  
767 June 2014. Donors were of self-assessed German origin. Allele frequencies were calculated to  
768 the two-field level (polypeptide sequence) (Schmidt et al., 2009). For allele frequency  
769 comparisons, chi-squared tests (Pearson, 1900) were applied in R (R Development Core Team,  
770 2011). Pairwise proportion tests were made between the allele or haplotype frequencies, where  $p$   
771  $< 0.05$  was considered significant. Omnibus tests for association with specific amino acid







- 845 Bos, K. I., Schuenemann, V. J., Golding, G. B., Burbano, H. A., Waglechner, N., Coombes,  
846 B. K., . . . Krause, J. (2011). A draft genome of *Yersinia pestis* from victims of the  
847 Black Death. *Nature*, *478*(7370), 506–510. doi:10.1038/nature10549
- 848 Boudreau, J. E., & Hsu, K. C. (2018). Natural Killer Cell Education and the Response to  
849 Infection and Cancer Therapy: Stay Tuned. *Trends Immunol*, *39*(3), 222–239.  
850 doi:10.1016/j.it.2017.12.001
- 851 Bowsky, W. M. (1971). *The Black Death: a turning point in history?*: New York, Holt,  
852 Rinhart and Winston.
- 853 Briggs, A. W., Stenzel, U., Johnson, P. L., Green, R. E., Kelso, J., Prufer, K., . . . Paabo, S.  
854 (2007). Patterns of damage in genomic DNA sequences from a Neandertal. *Proceedings*  
855 *of the National Academy of Sciences of the United States of America*, *104*(37), 14616–  
856 14621.
- 857 Büntgen, U., Ginzler, C., Esper, J., Tegel, W., & McMichael, A. J. (2012). Digitizing  
858 historical plague. *Clin. Infect. Dis.*, *55*(11), 1586–1588.
- 859 Cao, K., Hollenbach, J., Shi, X., Shi, W., Chopek, M., & Fernández-Viña, M. A. (2001).  
860 Analysis of the frequencies of HLA-A, B, and C alleles and haplotypes in the five  
861 major ethnic groups of the United States reveals high levels of diversity in these loci  
862 and contrasting distribution patterns in these populations. *Hum. Immunol.*, *62*(9),  
863 1009–1030.
- 864 Cedzynski, M., Nuytinck, L., Atkinson, A. P. M., St Swierzko, A., Zeman, K., Szemraj,  
865 J., . . . Kilpatrick, D. C. (2007). Extremes of L-ficolin concentration in children with  
866 recurrent infections are associated with single nucleotide polymorphisms in the FCN2  
867 gene. *Clin. Exp. Immunol.*, *150*(1), 99–104.
- 868 Clouse, M. (2002). *The Black Death Transformed: Disease and Culture in Early Renaissance*  
869 *Europe.*: Samuel K Cohn Jr. London and New York: Arnold and Oxford University  
870 Press, 2002, pp. 318, US\$65.00 (HB) ISBN: 0-340-70646-5. *International Journal of*  
871 *Epidemiology*, *31*(6), 1280–1281. doi:10.1093/ije/31.6.1280
- 872 Cohn, S. K., Jr. (2003). *The Black Death Transformed: Disease and Culture in Early*  
873 *Renaissance Europe.* London: Edward Arnold.
- 874 Danecek, P., Auton, A., Abecasis, G., Albers, C. A., Banks, E., DePristo, M. A., . . .  
875 Genomes Project Analysis, G. (2011). The variant call format and VCFtools.  
876 *Bioinformatics*, *27*(15), 2156–2158.
- 877 Darke, C., Guttridge, M. G., Thompson, J., MacNamara, S., Street, J., & Thomas, M. (1998).  
878 HLA class I (A, B) and II (DR, DQ) gene and haplotype frequencies in blood donors  
879 from Wales. *Exp Clin Immunogenet*, *15*, 69–83.
- 880 Dean, M., Carrington, M., Winkler, C., Huttley, G. A., Smith, M. W., Allikmets, R., . . .  
881 O'Brien, S. J. (1996). Genetic restriction of HIV-1 infection and progression to AIDS  
882 by a deletion allele of the *CCR5* structural gene. Hemophilia Growth and Development  
883 Study, Multicenter AIDS Cohort Study, Multicenter Hemophilia Cohort Study, San  
884 Francisco City Cohort, ALIVE Study. *Science*, *273*(5283), 1856–1862.
- 885 Di Marco, M., Schuster, H., Backert, L., Ghosh, M., Rammensee, H. G., & Stevanovic, S.

- 886 (2017). Unveiling the Peptide Motifs of HLA-C and HLA-G from Naturally Presented  
887 Peptides and Generation of Binding Prediction Matrices. *J Immunol*, 199(8), 2639–  
888 2651. doi:10.4049/jimmunol.1700938
- 889 Doherty, P. C., & Zinkernagel, R. M. (1975). A biological role for the major histocompatibility  
890 antigens. *Lancet*, 1(7922), 1406–1409.
- 891 Drummond, W. K., Nelson, C. A., Fowler, J., Epton, E. E., Mead, P. S., & Lawaczeck, E. W.  
892 (2014). Plague in a Pediatric Patient: Case Report and Use of Polymerase Chain  
893 Reaction as a Diagnostic Aid. *J Pediatric Infect Dis Soc*, 3(4), e38–41.  
894 doi:10.1093/jpids/piu001
- 895 Dubaniewicz, A., Lewko, B., Moszkowska, G., Zamorska, B., & Stepinski, J. (2000).  
896 Molecular subtypes of the HLA-DR antigens in pulmonary tuberculosis. *Int. J. Infect.*  
897 *Dis.*, 4(3), 129–133.
- 898 Dunne, C., Crowley, J., Hagan, R., Rooney, G., & Lawlor, E. (2008). HLA-A, B, Cw, DRB1,  
899 DQB1 and DPB1 alleles and haplotypes in the genetically homogenous Irish  
900 population. *Int. J. Immunogenet.*, 35(4–5), 295–302.
- 901 Ell, S. R. (1984). Immunity as a Factor in the Epidemiology of Medieval Plague. *Reviews of*  
902 *Infectious Diseases*, 6(6), 866–879. doi:10.1093/clinids/6.6.866
- 903 Ellwangen, S. (2007). *Die dunkle Zeit. Hexenverfolgung in der Stadt und Fürstpropstei*  
904 *Ellwangen*. Ellwangen: Stadtverwaltung Ellwangen.
- 905 Everitt, A. R., Clare S Fau – Pertel, T., Pertel T Fau – John, S. P., John Sp Fau – Wash, R.  
906 S., Wash Rs Fau – Smith, S. E., Smith Se Fau – Chin, C. R., . . . Kellam, P. (2012).  
907 IFITM3 restricts the morbidity and mortality associated with influenza. *Nature*,  
908 484(1476–4687 (Electronic)), 519–523. doi:D – NLM: EMS41068 FIR – Everingham, K
- 909 Excoffier, L., & Lischer, H. E. L. (2010). Arlequin suite ver 3.5: a new series of programs to  
910 perform population genetics analyses under Linux and Windows. *Mol Ecol Resour*,  
911 10(3), 564–567.
- 912 Faul, F., Erdfelder, E., Lang, A.-G., & Buchner, A. (2007). G\*Power 3: a flexible statistical  
913 power analysis program for the social, behavioral, and biomedical sciences. *Behav Res*  
914 *Methods*, 39(2), 175–191.
- 915 Feldman, M., Harbeck, M., Keller, M., Spyrou, M. A., Rott, A., Trautmann, B., . . . Krause,  
916 J. (2016). A High-Coverage *Yersinia pestis* Genome from a Sixth-Century Justinianic  
917 Plague Victim. *Mol. Biol. Evol.*, 33(11), 2911–2923.
- 918 Frisch, T., Sorensen, M. S., Overgaard, S., Lind, M., & Bretlau, P. (1998). Volume-Referent  
919 Bone Turnover Estimated From the Interlabel Area Fraction After Sequential Labeling.  
920 *Bone*, 22, 677–682. doi:10.1016/s8756-3282(98)00050-7
- 921 Fu, Q., Meyer, M., Gao, X., Stenzel, U., Burbano, H. A., Kelso, J., & Pääbo, S. (2013). DNA  
922 analysis of an early modern human from Tianyuan Cave, China. *Proc. Natl. Acad. Sci.*  
923 *U.S.A.*, 110(6), 2223–2227.
- 924 Fu, Q., Posth, C., Hajdinjak, M., Petr, M., Mallick, S., Fernandes, D., . . . Reich, D. (2016).  
925 The genetic history of Ice Age Europe. *Nature*, 534(7606), 200–205.
- 926 Galvani, A. P., & Slatkin, M. (2003). Evaluating plague and smallpox as historical selective

- 927 pressures for the CCR5–Delta 32 HIV–resistance allele. *Proceedings of the National*  
 928 *Academy of Sciences of the United States of America*, 100(25), 15276–15279.  
 929 doi:10.1073/pnas.2435085100
- 930 Gnirke, A., Melnikov, A., Maguire, J., Rogov, P., LeProust, E. M., Brockman, W., . . .  
 931 Nusbaum, C. (2009). Solution hybrid selection with ultra–long oligonucleotides for  
 932 massively parallel targeted sequencing. *Nat Biotech*, 27(2), 182–189.  
 933 doi:[http://www.nature.com/nbt/journal/v27/n2/supinfo/nbt.1523\\_S1.html](http://www.nature.com/nbt/journal/v27/n2/supinfo/nbt.1523_S1.html)
- 934 González–Neira, A., Calafell, F., Navarro, A., Lao, O., Cann, H., Comas, D., & Bertranpetit,  
 935 J. (2004). Geographic stratification of linkage disequilibrium: a worldwide population  
 936 study in a region of chromosome 22. *Hum. Genomics*, 1(6), 399–409.
- 937 Gravel, Henn, B., Gutenkunst, R., Indap, A., Marth, G., Clark, A., . . . Project, T. G.  
 938 (2011). Demographic history and rare allele sharing among human populations.  
 939 *Proceedings of the National Academy of Sciences of the United States of America*,  
 940 108(29), 11983–11988. doi:10.1073/pnas.1019276108
- 941 Guethlein, L. A., Norman, P. J., Hilton, H. G., & Parham, P. (2015). Co–evolution of MHC  
 942 class I and variable NK cell receptors in placental mammals. *Immunol. Rev.*, 267(1),  
 943 259–282.
- 944 Gumperz, J. E., Litwin, V., Phillips, J. H., Lanier, L. L., & Parham, P. (1995). The Bw4 public  
 945 epitope of HLA–B molecules confers reactivity with natural killer cell clones that  
 946 express NKB1, a putative HLA receptor. *J. Exp. Med.*, 181(3), 1133–1144.
- 947 Guo, Y., Patil, N. K., Luan, L., Bohannon, J. K., & Sherwood, E. R. (2018). The biology of  
 948 natural killer cells during sepsis. *Immunology*, 153(2), 190–202.  
 949 doi:10.1111/imm.12854
- 950 Haak, W., Lazaridis, I., Patterson, N., Rohland, N., Mallick, S., Llamas, B., . . . Reich, D.  
 951 (2015). Massive migration from the steppe was a source for Indo–European languages  
 952 in Europe. *Nature*, 522(7555), 207–211.
- 953 Haller, B. C., & Messer, P. W. (2017). SLiM 2: Flexible, Interactive Forward Genetic  
 954 Simulations. *Mol. Biol. Evol.*, 34(1), 230–240.
- 955 Haller, B. C., & Messer, P. W. (2019). SLiM 3: Forward Genetic Simulations Beyond the  
 956 Wright–Fisher Model. *Molecular Biology and Evolution*, 36(3), 632–637.  
 957 doi:10.1093/molbev/msy228
- 958 Hammer, C., Begemann, M., McLaren, P. J., Bartha, I., Michel, A., Klose, B., . . . Fellay, J.  
 959 (2015). Amino Acid Variation in HLA Class II Proteins Is a Major Determinant of  
 960 Humoral Response to Common Viruses. *American journal of human genetics*, 97(5),  
 961 738–743. doi:10.1016/j.ajhg.2015.09.008
- 962 Harrison, G. F., Sanz, J., Boulais, J., Mina, M. A.–O., Grenier, J. A.–O., Leng, Y., . . .  
 963 Barreiro, L. B. (2019). Natural selection contributed to immunological differences  
 964 between hunter–gatherers and agriculturalists. *Nature Ecology and Evolution*, 3(2397–  
 965 334X (Electronic)), 1253–1264.
- 966 Hellenthal, G., Busby, G. B., Band, G., Wilson, J. F., Capelli, C., Falush, D., & Myers, S.  
 967 (2014). A genetic atlas of human admixture history. *Science*, 343(6172), 747–751.

- 968 Hilton, H. G., Guethlein, L. A., Goyos, A. A.-O. X., Nemat-Gorgani, N., Bushnell, D. A.,  
 969 Norman, P. J., & Parham, P. (2015). Polymorphic HLA-C Receptors Balance the  
 970 Functional Characteristics of KIR Haplotypes. *J Immunol*, *195*(1550-6606  
 971 (Electronic)), 160-170.
- 972 Hoang, T. V., Toan, N. L., Song, L. H., Ouf, E. A., Bock, C. T., Kremsner, P. G., . . .  
 973 Velavan, T. P. (2011). Ficolin-2 levels and FCN2 haplotypes influence hepatitis B  
 974 infection outcome in Vietnamese patients. *PLoS ONE*, *6*(11), e28113.
- 975 Holdsworth, R., Hurley, C. K., Marsh, S. G., Lau, M., Noreen, H. J., Kempenich, J. H., . . .  
 976 Maier, M. (2009). The HLA dictionary 2008: a summary of HLA-A, -B, -C, -  
 977 DRB1/3/4/5, and -DQB1 alleles and their association with serologically defined HLA-  
 978 A, -B, -C, -DR, and -DQ antigens. *Tissue Antigens*, *73*(2), 95-170.  
 979 doi:10.1111/j.1399-0039.2008.01183.x
- 980 Hollenbach, J., Necedal, I., Ladner, M. B., Single, R. M., & Trachtenberg, E. A. (2012).  
 981 Killer cell immunoglobulin-like receptor (KIR) gene content variation in the HGDP-  
 982 CEPH populations. *Immunogenetics*. doi:10.1007/s00251-012-0629-x
- 983 Hollenbach, J., Norman, P. J., Creary, L. E., Damotte, V. A.-O., Montero-Martin, G.,  
 984 Caillier, S., . . . Oksenberg, J. R. (2019). A specific amino acid motif of HLA-DRB1  
 985 mediates risk and Interacts with smoking history in Parkinson's Disease. *Proc. Natl.*  
 986 *Acad. Sci. U.S.A.*, *116*(1091-6490 (Electronic)), 7419-7424.
- 987 Hummelshoj, T., Munthe-Fog, L., Madsen, H. O., Fujita, T., Matsushita, M., & Garred, P.  
 988 (2005). Polymorphisms in the FCN2 gene determine serum variation and function of  
 989 Ficolin-2. *Hum. Mol. Genet.*, *14*(12), 1651-1658.
- 990 Huson, D. H., Auch, A. F., Qi, J., & Schuster, S. C. (2007). MEGAN analysis of  
 991 metagenomic data. *Genome Res.*, *17*(3), 377-386.
- 992 Inohara, Chamailard, McDonald, C., & Nunez, G. (2005). NOD-LRR proteins: role in host-  
 993 microbial interactions and inflammatory disease. *Annu Rev Biochem*, *74*, 355-383.  
 994 doi:10.1146/annurev.biochem.74.082803.133347
- 995 Johansson, A., Ingman, M., Mack, S. J., Ehrlich, H., & Gyllensten, U. (2008). Genetic origin  
 996 of the Swedish Sami inferred from HLA class I and class II allele frequencies. *Eur J*  
 997 *Hum Genet.*, *16*, 1341-1349.
- 998 Jonsson, H., Ginolhac, A., Schubert, M., Johnson, P. L., & Orlando, L. (2013).  
 999 mapDamage2.0: fast approximate Bayesian estimates of ancient DNA damage  
 1000 parameters. *Bioinformatics*, *29*(13), 1682-1684.
- 1001 Kairies, M.-S. (2015). *Drei frühneuzeitliche Massengräber aus Ellwangen (Jagst) -*  
 1002 *Paläopathologie und demographische Struktur.* (Master of Science), University of  
 1003 Tübingen, Germany.
- 1004 Karlsson, E. K., Harris Jb Fau - Tabrizi, S., Tabrizi S Fau - Rahman, A., Rahman A Fau -  
 1005 Shlyakhter, I., Shlyakhter I Fau - Patterson, N., Patterson N Fau - O'Dushlaine,  
 1006 C., . . . Larocque, R. C. (2013). Natural selection in a bangladeshi population from the  
 1007 cholera-endemic ganges river delta. *Sci Transl Med.*, *5*(1946-6242 (Electronic)).
- 1008 Keller, M., Spyrou, M. A., Scheib, C. L., Neumann, G. U., Kröpelin, A., Haas-Gebhard,



1009 B., . . . Krause, J. (2019). Ancient genomes from across Western Europe reveal early  
1010 diversification during the First Pandemic (541–750). *Proc. Natl. Acad. Sci. U.S.A.*,  
1011 *116*(25), 12363–12372.

1012 Key, F. M., Fu, Q., Romagné, F., Lachmann, M., & Andrés, A. M. (2016). Human adaptation  
1013 and population differentiation in the light of ancient genomes. *Nat Commun*, *7*, 10775.

1014 Key, F. M., Peter, B., Dennis, M. Y., Huerta-Sánchez, E., Tang, W., Prokunina-Olsson,  
1015 L., . . . Andrés, A. M. (2014). Selection on a variant associated with improved viral  
1016 clearance drives local, adaptive pseudogenization of interferon lambda 4 (IFNL4).  
1017 (1553–7404 (Electronic)).

1018 Kim, S., Sunwoo, J. B., Yang, L., Choi, T., Song, Y.-J., French, A. R., . . . Yokoyama, W. M.  
1019 (2008). HLA alleles determine differences in human natural killer cell responsiveness  
1020 and potency. *Proceedings of the National Academy of Sciences of the United States of*  
1021 *America*, *105*(8), 3053–3058. doi:10.1073/pnas.0712229105

1022 Kircher, M., Sawyer, S., & Meyer, M. (2012). Double indexing overcomes inaccuracies in  
1023 multiplex sequencing on the Illumina platform. *Nucleic Acids Res*, *40*(1), e3.

1024 Klebanov, N. (2018). Genetic Predisposition to Infectious Disease. *Cureus*, *10*(8), e3210.

1025 Korneliussen, T. S., Albrechtsen, A., & Nielsen, R. (2014). ANGSD: Analysis of Next  
1026 Generation Sequencing Data. *BMC Bioinformatics*, *15*, 356.

1027 Kwiatkowski, D. P. (2005). How malaria has affected the human genome and what human  
1028 genetics can teach us about malaria. *Am. J. Hum. Genet.*, *77*(0002–9297 (Print)), 171–  
1029 192.

1030 Laayouni, H., Oosting, M., Luisi, P., Ioana, M., Alonso, S., Ricaño-Ponce, I., . . . Netea, M.  
1031 G. (2014). Convergent evolution in European and Roma populations reveals pressure  
1032 exerted by plague on Toll-like receptors. *Proc. Natl. Acad. Sci. U.S.A.*, *111*(7), 2668–  
1033 2673.

1034 Lamkanfi, M., & Dixit, V. M. (2014). Mechanisms and functions of inflammasomes. *Cell*,  
1035 *157*(5), 1013–1022. doi:10.1016/j.cell.2014.04.007

1036 Lamnidis, T. C., Majander, K., Jeong, C., Salmela, E., Wessman, A., Moiseyev, V., . . .  
1037 Schiffels, S. (2018). Ancient Fennoscandian genomes reveal origin and spread of  
1038 Siberian ancestry in Europe. *Nat Commun*, *9*(1), 5018. doi:10.1038/s41467-018-  
1039 07483-5

1040 Lazaridis, I., Patterson, N., Mittnik, A., Renaud, G., Mallick, S., Kirsanow, K., . . . Krause,  
1041 J. (2014). Ancient human genomes suggest three ancestral populations for present-day  
1042 Europeans. *Nature*, *513*(7518), 409–413.

1043 Lenski, R. E. (1988). Evolution of plague virulence. *Nature*, *334*(6182), 473–474.

1044 Li, H. (2011). A statistical framework for SNP calling, mutation discovery, association  
1045 mapping and population genetical parameter estimation from sequencing data.  
1046 *Bioinformatics*, *27*(21), 2987–2993.

1047 Li, H., & Durbin, R. (2010). Fast and accurate long-read alignment with Burrows-Wheeler  
1048 transform. *Bioinformatics*, *26*(5), 589–595.

1049 Li, H., Handsaker, B., Wysoker, A., Fennell, T., Ruan, J., Homer, N., . . . Genome Project



- 1050 Data Processing, S. (2009). The Sequence Alignment/Map format and SAMtools.  
1051 *Bioinformatics*, 25(16), 2078–2079.
- 1052 Lindo, J., Huerta-Sánchez, E., Nakagome, S., Rasmussen, M., Petzelt, B., Mitchell, J., . . .  
1053 Malhi, R. S. (2016). A time transect of exomes from a Native American population  
1054 before and after European contact. *Nat Commun*, 7, 13175.
- 1055 Lipatov, M., Sanjeev, K., Patro, R., & Veeramah, K. (2015). Maximum Likelihood Estimation  
1056 of biological Relatedness from low Coverage Sequencing Data. *bioRxiv*.
- 1057 Long, E. O., Kim, H. S., Liu, D., Peterson, M. E., & Rajagopalan, S. (2013). Controlling  
1058 natural killer cell responses: integration of signals for activation and inhibition. *Annu  
1059 Rev Immunol*, 31, 227–258. doi:10.1146/annurev-immunol-020711-075005
- 1060 Luo, F., Sun, X., Wang, Y., Wang, Q., Wu, Y., Pan, Q., . . . Zhang, X.-L. (2013). Ficolin-2  
1061 defends against virulent Mycobacteria tuberculosis infection in vivo, and its  
1062 insufficiency is associated with infection in humans. *PLoS ONE*, 8(9), e73859.
- 1063 Martinon, F., Burns, K., & Tschopp, J. (2002). The inflammasome: a molecular platform  
1064 triggering activation of inflammatory caspases and processing of proIL-β. *Mol Cell*,  
1065 10(2), 417–426.
- 1066 Mathieson, I., Lazaridis, I., Rohland, N., Mallick, S., Patterson, N., Roodenberg, S. A., . . .  
1067 Reich, D. (2015). Genome-wide patterns of selection in 230 ancient Eurasians. *Nature*,  
1068 528(7583), 499–503.
- 1069 McManus, K. A.-O., Taravella, A. M., Henn, B. A.-O. X., Bustamante, C. D., Sikora, M., &  
1070 Cornejo, O. A.-O. (2017). Population genetic analysis of the DARC locus (Duffy)  
1071 reveals adaptation from standing variation associated with malaria resistance in  
1072 humans. *PLoS Genet*, 13(1553–7404 (Electronic)).
- 1073 McVicker, G., Gordon, D., Davis, C., & Green, P. (2009). Widespread genomic signatures of  
1074 natural selection in hominid evolution. *PLoS Genet.*, 5(5), e1000471.
- 1075 Meyer, M., & Kircher, M. (2010). Illumina sequencing library preparation for highly  
1076 multiplexed target capture and sequencing. *Cold Spring Harb Protoc*, 2010(6),  
1077 pdb.prot5448.
- 1078 Monroy, K., Jose, M., Jakobsson, M., & Günther, T. (2017). Estimating genetic Kin  
1079 Relationships in prehistoric Populations. *bioRxiv*.
- 1080 Morelli, G., Song, Y., Mazzoni, C. J., Eppinger, M., Roumagnac, P., Wagner, D. M., . . .  
1081 Achtman, M. (2010). Yersinia pestis genome sequencing identifies patterns of global  
1082 phylogenetic diversity. *Nat. Genet.*, 42(12), 1140–1143.
- 1083 Namouchi, A., Guellil, M., Kersten, O., Hänsch, S., Ottoni, C., Schmid, B. V., . . . Bramanti,  
1084 B. (2018). Integrative approach using Yersinia pestis genomes to revisit the historical  
1085 landscape of plague during the Medieval Period. *Proceedings of the National Academy  
1086 of Sciences*, 115(50), E11790. doi:10.1073/pnas.1812865115
- 1087 Neefjes, J., Jongsma, M. L. M., Paul, P., & Bakke, O. (2011). Towards a systems  
1088 understanding of MHC class I and MHC class II antigen presentation. *Nat. Rev.  
1089 Immunol.*, 11(12), 823–836.
- 1090 Norman, P. J., Hollenbach, J., Nemat-Gorgani, N., Marin, W., Norberg, S., Ashouri, E., . . .



- 1132 *Cell Host Microbe*, 3(6), 399–407.
- 1133 Pingel, J., Solloch, U. V., Hofmann, J. A., Lange, V., Ehninger, G., & Schmidt, A. H. (2013).  
 1134 High-resolution HLA haplotype frequencies of stem cell donors in Germany with  
 1135 foreign parentage: how can they be used to improve unrelated donor searches? *Hum.*  
 1136 *Immunol.*, 74(3), 330–340.
- 1137 Pinhasi, R., Fernandes, D., Sirak, K., Novak, M., Connell, S., Alpaslan-Roodenberg, S., . . .  
 1138 Hofreiter, M. (2015). Optimal Ancient DNA Yields from the Inner Ear Part of the  
 1139 Human Petrous Bone. *PLoS ONE*, 10(6), e0129102. doi:10.1371/journal.pone.0129102
- 1140 Politzer, R., & WHO. (1954). *Plague*.
- 1141 Prugnolle, F., Manica, A., Charpentier, M., Guégan, J., V., G., & Balloux, F. (2005).  
 1142 Pathogen-driven selection and worldwide HLA class I diversity. *Current Biology*, 15,  
 1143 1022–1027.
- 1144 Quinlan, A. R. (2014). BEDTools: The Swiss-Army Tool for Genome Feature Analysis. *Curr*  
 1145 *Protoc Bioinformatics*, 47, 11.12.11–34. doi:10.1002/0471250953.bi1112s47
- 1146 Quintana-Murci, L. (2019). Human Immunology through the Lens of Evolutionary Genetics.  
 1147 *Cell*, 177(1), 184–199. doi:10.1016/j.cell.2019.02.033
- 1148 R Development Core Team. (2011). *R: A Language and Environment for Statistical*  
 1149 *Computing. Vienna, Austria : the R Foundation for Statistical Computing: R*  
 1150 *Foundation for Statistical Computing*.
- 1151 Radwan, J., Babik, W., Kaufman, J., Lenz, T. L., & Winternitz, J. (2020). Advances in the  
 1152 Evolutionary Understanding of MHC Polymorphism. *Trends in Genetics*, 36, 298–311.
- 1153 Ralph, P. L., & Coop, G. (2015). Convergent Evolution During Local Adaptation to Patchy  
 1154 Landscapes. *PLoS Genet.*, 11(11), e1005630.
- 1155 Rascovan, N., Sjögren, K.-G., Kristiansen, K., Nielsen, R., Willerslev, E., Desnues, C., &  
 1156 Rasmussen, S. (2019). Emergence and Spread of Basal Lineages of *Yersinia pestis*  
 1157 during the Neolithic Decline. *Cell*, 176(1–2), 295–305.e210.
- 1158 Rasmussen, S., Allentoft, M. E., Nielsen, K., Orlando, L., Sikora, M., Sjogren, K. G., . . .  
 1159 Willerslev, E. (2015). Early divergent strains of *Yersinia pestis* in Eurasia 5,000 years  
 1160 ago. *Cell*, 163(3), 571–582. doi:10.1016/j.cell.2015.10.009
- 1161 Renaud, G., Slon, V., Duggan, A. T., & Kelso, J. (2015). Schmutzi: estimation of  
 1162 contamination and endogenous mitochondrial consensus calling for ancient DNA.  
 1163 *Genome Biology*, 16(1), 224. doi:10.1186/s13059-015-0776-0
- 1164 Robinson, J., Halliwell, J. A., Hayhurst, J. D., Flicek, P., Parham, P., & Marsh, S. G. E.  
 1165 (2015). The IPD and IMGT/HLA database: allele variant databases. *Nucleic Acids*  
 1166 *Res.*, 43(Database issue), D423–D431.
- 1167 Robinson, J., Thorvaldsdóttir, H., Winckler, W., Guttman, M., Lander, E. S., Getz, G., &  
 1168 Mesirov, J. P. (2011). Integrative genomics viewer. *Nat. Biotechnol.*, 29(1), 24–26.
- 1169 Rohland, N., Harney, E., Mallick, S., Nordenfelt, S., & Reich, D. (2015). Partial uracil-DNA-  
 1170 glycosylase treatment for screening of ancient DNA. *Philos Trans R Soc Lond B Biol*  
 1171 *Sci*, 370(1660), 20130624. doi:10.1098/rstb.2013.0624
- 1172 Rohland, N., & Hofreiter, M. (2007). Ancient DNA extraction from bones and teeth. *Nat*

- 1173 *Protoc*, 2(7), 1756–1762.
- 1174 Sabeti, Schaffner, S., Fry, B., Lohmueller, J., Varilly, P., Shamovsky, O., . . . Lander, E. S.  
 1175 (2006). Positive natural selection in the human lineage. *Science*, 312(5780), 1614–  
 1176 1620. doi:10.1126/science.1124309
- 1177 Sabeti, Varilly, P., Fry, B., Lohmueller, J., Hostetter, E., Cotsapas, C., . . . Stewart, J.  
 1178 (2007). Genome-wide detection and characterization of positive selection in human  
 1179 populations. *Nature*, 449(1476–4687 (Electronic)), 913–918. doi:D – NLM: UKMS4416  
 1180 EDAT– 2007/10/19 09:00 MHDA– 2007/12/06 09:00 CRDT– 2007/10/19 09:00  
 1181 PHST– 2007/08/08 00:00 [received] PHST– 2007/09/13 00:00 [accepted] PHST–  
 1182 2007/10/19 09:00 [pubmed] PHST– 2007/12/06 09:00 [medline] PHST– 2007/10/19  
 1183 09:00 [entrez] AID – nature06250 [pii] AID – 10.1038/nature06250 [doi] PST –  
 1184 ppublish
- 1185 Saunders, P. M., Vivian, J. P., O’Connor, G. M., Sullivan, L. C., Pymm, P., Rossjohn, J., &  
 1186 Brooks, A. G. (2015). A bird’s eye view of NK cell receptor interactions with their  
 1187 MHC class I ligands. *Immunol Rev*, 267(1), 148–166. doi:10.1111/imr.12319
- 1188 Schmidt, A. H., Baier, D., Solloch, U. V., Stahr, A., Cereb, N., Wassmuth, R., . . . Rutt, C.  
 1189 (2009). Estimation of high-resolution HLA-A, -B, -C, -DRB1 allele and haplotype  
 1190 frequencies based on 8862 German stem cell donors and implications for strategic  
 1191 donor registry planning. *Hum. Immunol.*, 70(11), 895–902.
- 1192 Skoglund, P., Storå, J., Götherström, A., & Jakobsson, M. (2013). Accurate sex identification  
 1193 of ancient human remains using DNA shotgun sequencing. *Journal of Archaeological  
 1194 Science*, 40(12), 4477–4482.
- 1195 Solloch, U. V., Lang, K., Lange, V., Böhme, I., Schmidt, A. H., & Sauter, J. (2017).  
 1196 Frequencies of gene variant CCR5-Δ32 in 87 countries based on next-generation  
 1197 sequencing of 1.3 million individuals sampled from 3 national DKMS donor centers.  
 1198 *Hum. Immunol.*, 78(11–12), 710–717.
- 1199 Spyrou, M. A., Keller, M., Tikhbatova, R. I., Scheib, C. L., Nelson, E. A., Andrades  
 1200 Valtueña, A., . . . Krause, J. (2019). Phylogeography of the second plague pandemic  
 1201 revealed through analysis of historical *Yersinia pestis* genomes. *Nature  
 1202 Communications*, 10(1), 4470–4470. doi:10.1038/s41467-019-12154-0
- 1203 Spyrou, M. A., Tikhbatova, R. I., Feldman, M., Drath, J., Kacki, S., Beltran de Heredia,  
 1204 J., . . . Krause, J. (2016). Historical *Y. pestis* Genomes Reveal the European Black  
 1205 Death as the Source of Ancient and Modern Plague Pandemics. *Cell Host Microbe*,  
 1206 19(6), 874–881. doi:10.1016/j.chom.2016.05.012
- 1207 Spyrou, M. A., Tikhbatova, R. I., Wang, C.-C., Valtueña, A. A., Lankapalli, A. K.,  
 1208 Kondrashin, V. V., . . . Krause, J. (2018). Analysis of 3800-year-old *Yersinia pestis*  
 1209 genomes suggests Bronze Age origin for bubonic plague. *Nat Commun*, 9(1), 2234.
- 1210 Stephens, J. C., Reich, D. E., Goldstein, D. B., Shin, H. D., Smith, M. W., Carrington,  
 1211 M., . . . Dean, M. (1998). Dating the origin of the CCR5-Delta32 AIDS-resistance  
 1212 allele by the coalescence of haplotypes. *Am. J. Hum. Genet.*, 62(6), 1507–1515.
- 1213 Sun, J., Yang, C., Fei, W., Zhang, X., Sheng, Y., Zheng, X., . . . Zhang, X. (2018). HLA-









1287 analyses. PJN, WHP and GFH performed simulations for natural selection. JS, US and AHS  
1288 contributed the DKMS allele frequencies. RW and SA led the Excavation in Ellwangen. JW and  
1289 RW provided the 16<sup>th</sup> century Ellwangen samples. MSK and JW conducted anthropological  
1290 analyses. AI, JH, PJN and JK wrote the manuscript. JK led the study.

1291

### 1292 **Conflicts of Interests**

1293 The authors declare no conflicts of interests.

1294

### 1295 **Data Availability**

1296 The data underlying this article is available on the European Nucleotide Archive under the  
1297 accession number PRJEB44124 (ERP128137).

1298

1299

1300

1301

1302

1303

1304

1305

1306

1307

1308

1309

1310

1311

1312

1313

1314

1315

1316

1317 **Figures**

1318



1319

1320

1321 **Figure 1. Mass burials discovered at Ellwangen. A.** Location of Ellwangen in Germany. **B.**

1322 Location of the marketplace, where the mass burials were discovered during an excavation in

1323 2013-2015. **C.** Mass grave 549 showing several individuals being buried together.

1324

1325

1326

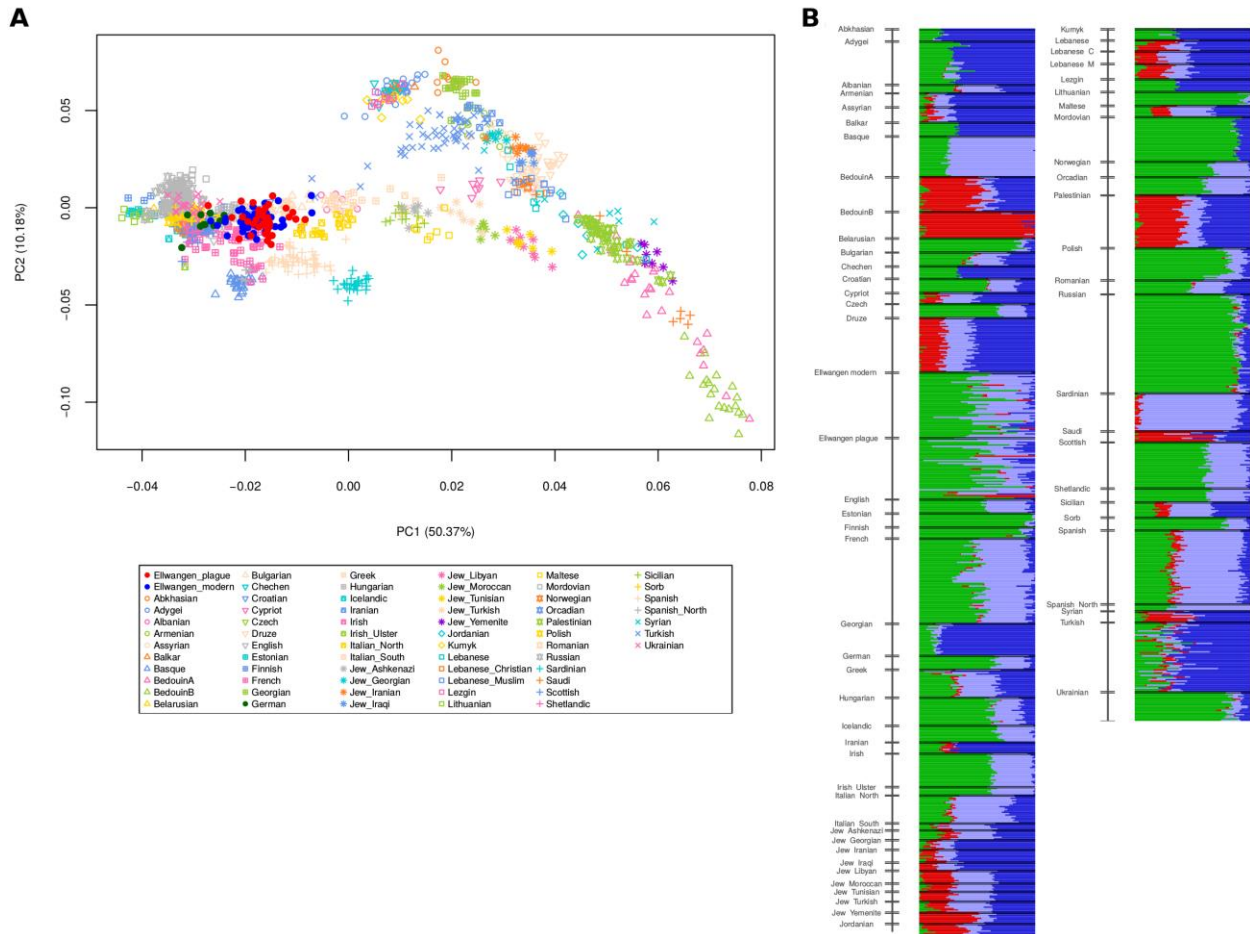
1327

1328

1329

1330

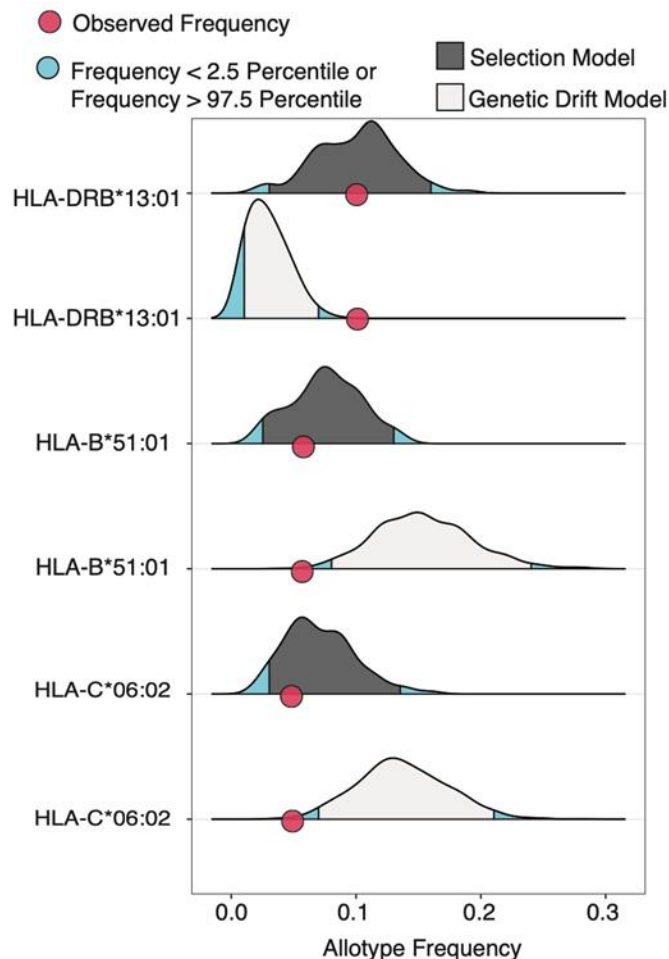
1331



1332  
 1333  
 1334  
 1335  
 1336  
 1337  
 1338  
 1339  
 1340  
 1341  
 1342  
 1343  
 1344  
 1345  
 1346

**Figure 2. The 16<sup>th</sup> century plague victims and modern inhabitants of Ellwangen form a continuous population**

**A.** PCA showing the 16<sup>th</sup> century (red) and modern (blue) Ellwangen populations in the context of 65 modern day populations from West-Eurasia based on 1,233,013 genome wide SNPs (Lazaridis et al. 2014; Haak et al. 2015; Fu et al. 2016). **B.** Admixture modeling based on four ancestral components (K=4) of the same 65 modern West Eurasian populations including 16<sup>th</sup> century (Ellwangen plague) and modern Ellwangen (Ellwangen modern) populations. The K=4 model was chosen due to the lowest cross-validation error.



1347

1348 **Figure 3. Natural selection drives HLA allele frequency changes**

1349 Density plots showing the distributions of allele frequencies from SLIM3 model simulations with  
 1350 (dark grey) or without (light grey) natural selection. The starting frequency for simulations was  
 1351 the observed frequency in the 16<sup>th</sup> century population. Selection coefficients for the models with  
 1352 natural selection were -0.1 for *HLA-B\*51:01* and *HLA-C\*06:02* and 0.2 for *DRB1\*13:01*  
 1353 (Supplementary Figure 5). The 2.5% extremes are shown in blue illustrating where the p-value  
 1354 cut-off of 0.05 would occur. Red points represent the frequency in the modern-day population.

1355

1356

1357 **Table 1.** Genes identified in the 0.01% tail of distribution following *DAnC* analysis. **Ref** =  
 1358 reference, **Alt** = alternative, **Der** = derived, **Anc** = derived allele frequency in Ellwangen 16<sup>th</sup>  
 1359 century, **Mod** = derived allele frequency in Ellwangen modern, **CEU** = derived allele frequency  
 1360 in Central Europeans from Utah, **FIN** = derived allele frequency in Finnish, **GBR** = derived

1361 allele frequency in Great Britains (obtained from the 1000 Genomes Project Phase 3 data). Red  
 1362 text indicates alleles that have significantly ( $p < 0.05$ ) increased in frequency in the modern  
 1363 individuals and blue text indicates that allele frequency has significantly ( $p < 0.05$ ) decreased in  
 1364 frequency in the modern individuals.  $F_{ST}$  empirical p-value refers to the empirical distribution of  
 1365  $F_{ST}$  calculated between the 16<sup>th</sup> century and the modern Ellwangen population.  
 1366

Chromosome			Allele			Ellwangen											
No.	Position	SNP ID	Ref	Alt	Der	Anc	Mod	CEU	FIN	GBR	DAnc	$F_{ST}$ empirical p-value	Variant	Gene	Function		
9	137772664	rs17514136	A	G	G	0.17	0.37	0.28	0.24	0.21	0.20	0.99	5_prime_UTR	FCN2	activation of the lectin complement pathway		
9	137779026	rs17549193	C	T	T	0.19	0.39	0.29	0.25	0.23	0.20	0.99	missense	FCN2			
11	7079038	rs10839708	G	A	A	0.69	0.51	0.60	0.65	0.63	0.18	0.97	missense	NLRP14	activation of pro- inflammatory caspases		

1367  
 1368 **Table 2.** Genotype and allele frequencies of *CCR5*-wildtype (wt), and *CCR5-Δ32* ( $\Delta 32$ ), among  
 1369 the plague victims and modern individuals from Ellwangen. The individual genotypes are given  
 1370 in Supplementary Data 6A. The frequencies for Germany were obtained from a study of German  
 1371 bone marrow donor registry volunteers (Solloch et al., 2017) for comparison.  
 1372

	Genotype frequency (%)			Allele Frequency (%)	
	wt/wt	wt/ $\Delta 32$	$\Delta 32/\Delta 32$	wt	$\Delta 32$
<b>Ellwangen plague</b>	71.4	23.8	4.8	83.4	16.6
<b>Ellwangen modern</b>	78.4	21.6	0	89.2	10.8
<b>Germany</b>	79.2	19.4	1.4	88.8	11.2

1373  
 43



1374 **Table 3.** *HLA-B*, *-C* and *-DRB1* allele frequencies in 16<sup>th</sup> century plague victims and modern  
 1375 inhabitants of Ellwangen. Frequency differences with  $p < 0.05$  are highlighted in red. No  
 1376 significance could be obtained after multiple testing correction (for details see Supplementary  
 1377 Data 5A).

Locus	Frequency (%)	Frequency (%)	P-value
	Plague	Modern	
B*07:02	13.89	14	0.984
B*08:01	9.72	13	0.508
B*13:02	1.39	3	0.490
B*14:02	1.39	4	0.315
B*15:01	5.56	10	0.294
B*18:01	5.56	3	0.402
B*27:05	4.17	3	0.680
B*35:01	4.17	6	0.595
B*35:03	4.17	2	0.403
B*38:01	2.78	1	0.379
B*40:01	4.17	2	0.403
B*44:02	4.17	6	0.595
B*49:01	1.39	1	0.814
B*50:01	4.17	1	0.174
<b>B*51:01</b>	<b>15.28</b>	<b>6</b>	<b>0.044</b>
B*52:01	1.39	1	0.814
B*57:01	4.17	2	0.403
C*01:02	4.17	2	0.403
C*02:02	4.17	3	0.680
C*03:03	4.17	11	0.106
C*03:04	6.94	4	0.393
C*04:01	11.11	15	0.460
C*05:01	2.78	5	0.467
<b>C*06:02</b>	<b>13.89</b>	<b>5</b>	<b>0.041</b>
C*07:01	13.89	17	0.580
C*07:02	15.28	12	0.533
C*07:04	1.39	1	0.814
C*08:02	1.39	4	0.315
C*12:02	1.39	1	0.814
C*12:03	5.56	5	0.871
C*15:02	5.56	4	0.632
DRB1*01:01	9.72	7	0.520
DRB1*01:02	1.39	2	0.763
DRB1*03:01	11.11	11	0.982
DRB1*04:01	9.72	3	0.063
DRB1*04:07	1.39	1	0.814
DRB1*04:08	1.39	2	0.763
DRB1*07:01	11.11	12	0.857
DRB1*09:01	1.39	2	0.763
DRB1*11:01	9.72	6	0.363
DRB1*11:03	2.78	2	0.738
DRB1*11:04	1.39	4	0.315
DRB1*12:01	1.39	1	0.814
DRB1*13:01	2.78	10	0.067
DRB1*13:02	2.78	6	0.323
DRB1*15:01	18.06	15	0.592
DRB1*15:02	1.39	1	0.814
DRB1*16:01	1.39	3	0.490
DRB1*01	11.11	9	0.625
DRB1*03	11.11	11	0.956
DRB1*04	15.28	10	0.281
DRB1*07	11.11	12	0.883
DRB1*11	13.89	13	0.838
<b>DRB1*13</b>	<b>5.56</b>	<b>17</b>	<b>0.026</b>
DRB1*15	19.44	16	0.529

1378

1379



1380 **Table 4. A.** Allele frequencies for (top) presence of *KIR3DL1* gene, (bottom) *KIR3DL1* alleles  
 1381 (‡) indicates allele not expressed at the cell surface (Guethlein et al., 2015).

1382 **B.** Genotype frequencies for *KIR3DL1* and *I80<sup>+</sup>HLA-B* in 16<sup>th</sup> century (plague) and modern  
 1383 inhabitants of Ellwangen. Shown are p values from (chi) chi square, and (lme) logistic mixed  
 1384 effects model.

1385  
 1386

<b>A</b>		<b>frequency plague</b>	<b>frequency modern</b>
<b>Gene</b>	<i>KIR3DL1</i>	0.81	0.74
	*00101	0.25	0.18
	*002	0.17	0.13
<b>Alleles</b>	*00401‡	0.11	0.08
	*00501	0.13	0.18
	*007	0.03	0.02
	*008	0.07	0.04
	*01502	0.06	0.11

<b>B</b>	<b>Genotype</b>	<b>Number Observed</b>		<b>p=</b>	
		<b>plague (N=36)</b>	<b>modern (N=50)</b>	<b>(chi)</b>	<b>(lme)</b>
	<i>I-80<sup>+</sup>HLA-B</i>	20 (55.6%)	16 (32%)	0.029	0.07
	<i>KIR3DL1</i>	35 (97.2%)	44 (88%)	0.099	0.29
	<i>KIR3DL1 + I-80<sup>+</sup>HLA-B</i>	19 (52.8%)	13 (26%)	0.011	0.01

1387